Elucidation of the Structure and Synthesis of Neuroprotective Low Molecular Mass Components of the Parawixia bistriata Spider Venom

Forster, Yvonne M ; Green, Jennifer Leigh ; Khatiwada, Apeksha ; Liberato, José Luiz ; Narayana Reddy, Poli Adi ; Salvino, Joseph M ; Bienz, Stefan ; Bigler, Laurent ; dos Santos, Wagner Ferreira ; Karklin Fontana, Andréia Cristina

Abstract: The South American social spider Parawixia bistriata produces a venom containing complex organic compounds with intriguing biological activities. The crude venom leads to paralysis in termites and stimulates l-glutamate uptake and inhibits GABA uptake in rat brain synaptosomes. Glutamate is the major neurotransmitter at the insect neuromuscular junction and at the mammalian central nervous system, suggesting a modulation of the glutamatergic system by the venom. Parawixin1, 2, and 10 (Pwx1, 2 and 10) are HPLC fractions that demonstrate this bioactivity. Pwx1 stimulates l-glutamate uptake through the main transporter in the brain, EAAT2, and is neuroprotective in in vivo glaucoma models. Pxw2 inhibits GABA and glycine uptake in synaptosomes and inhibits seizures and neurodegeneration, and Pwx10 increases l-glutamate uptake in synaptosomes and is neuroprotective and anticonvulsant, shown in in vivo epilepsy models. Herein, we investigated the low molecular mass compounds in this venom and have found over 20 small compounds and 36 unique acylpolyamines with and without amino acid linkers. The active substances in fractions Pwx1 and Pwx2 require further investigation. We elucidated and confirmed the structure of the active acylpolyamine in Pwx10. Both fraction Pwx10 and the synthesized component enhance the activity of transporters EAAT1 and EAAT2, and, importantly, offer in vitro neuroprotection against excitotoxicity in primary cultures. These data suggest that compounds with this mechanism could be developed into therapies for disorders in which l-glutamate excitotoxicity is involved.

DOI: https://doi.org/10.1021/acschemneuro.0c00007

ACS Chemical Neuroscience

Article

Elucidation of the structure and synthesis of neuroprotective low molecular mass components of the *Parawixia bistriata* spider venom

Yvonne M. Forster, Jennifer Leigh Green, Apeksha Khatiwada, José Luiz Liberato, Poli Adi Narayana Reddy, Joseph M. Salvino, Stefan Bienz, Laurent Bigler, Wagner Ferreira dos Santos, and Andreia Cristina Karklin Fontana

ACS Chem. Neurosci., **Just Accepted Manuscript** • DOI: 10.1021/acschemneuro.0c00007 • Publication Date (Web): 28 Apr 2020

Just Accepted

is published by the American Chemical Society. 1155 Sixteenth Street N.W., Washington, DC 20036

Elucidation of the structure and synthesis of neuroprotective low molecular mass components of the *Parawixia bistriata* spider venom

Yvonne M. Forster[a], Jennifer Leigh Green[b], Apeksha Khatiwada[b], José Luiz Liberato[c], Poli Adi Narayana Reddy[d], Joseph M. Salvino[d], Stefan Bienz[a], Laurent Bigler[a], Wagner Ferreira dos Santos[c*], Andréia Cristina Karklin Fontana[b*]

[a]Department of Chemistry, University of Zurich, Zurich, CH 8057, Switzerland

[b]Department of Pharmacology and Physiology, Drexel University College of Medicine, Philadelphia, PA, 19102, United States

[c]Department of Biology, University of São Paulo, Ribeirão Preto, SP, 14040-900, Brazil

[d]The Wistar Institute, Philadelphia, PA, 19104, United States

***Co-corresponding authors:**

*Andréia C. K. Fontana

Department of Pharmacology and Physiology, Drexel University College of Medicine, Philadelphia, PA, 19102, United States

Tel: +1 215-762-4399. E-mail: acm83@drexel.edu

*Wagner F. dos Santos

Department of Biology, University of São Paulo

Ribeirão Preto, São Paulo, SP, 14040-900, Brazil

Tel: +55 16-3315-3657. E-mail: wagnerf@usp.br

Abstract

The South-American social spider *Parawixia bistriata* produces a venom containing complex organic compounds with intriguing biological activities. The crude venom leads to paralysis in termites and stimulates L-glutamate uptake and inhibits GABA uptake in rat brain synaptosomes. Glutamate is the major neurotransmitter at the insect neuromuscular junction and at the mammalian central nervous system, suggesting a modulation of the glutamatergic system by the venom. Parawixin1, 2, and 10 (Pwx1, 2 and 10) are HPLC fractions that demonstrate this bioactivity. Pwx1 stimulates L-glutamate uptake through the main transporter in the brain, EAAT2, and is neuroprotective in *in vivo* glaucoma models. Pxw2 inhibits GABA and glycine uptake in synaptosomes and inhibits seizures and neurodegeneration, and Pwx10 increases L-glutamate uptake in synaptosomes and is neuroprotective and anticonvulsant, shown in *in vivo* epilepsy models. Herein, we investigated the low molecular mass compounds in this venom and have found over 20 small compounds and 36 unique acylpolyamines with and without amino acid linkers. The active substances in fractions Pwx1 and Pwx2 require further investigation. We elucidated and confirmed the structure of the active acylpolyamine in Pwx10. Both, fraction Pwx10 and the synthesized component enhance the activity of transporters EAAT1 and EAAT2, and importantly, offer *in vitro* neuroprotection against excitotoxicity in primary cultures. This data suggests that compounds with this mechanism could be developed into therapies for disorders in which L-glutamate excitotoxicity is involved.

Keywords: acylpolyamine, Parawixin10 (Pwx10), UHPLC, high-resolution MS, MS/MS, neurotransmitter, GABA, EAAT1, EAAT2, neuroprotection.

Introduction

The spider *Parawixia bistriata* (Araneae; Araneidae) is a colonial orb-weaver species, found in the Southeast of Brazil, the North of Argentina, and Paraguay. The bioactivity of the *P. bistriata* venom was intensively studied by the group of *Ferreira dos Santos*. In 2000, it was shown that the venom, injected into termites, leads to irreversible and dose-dependent paralysis[1]. As L-glutamate serves as the major neurotransmitter at the insect neuromuscular junction[2-3], these results indicated that the venom might mediate its action through the effects on the glutamatergic system. Additional *in vitro* studies showed that the crude venom stimulates L-glutamate uptake and inhibits γ-amino butyric acid (GABA) uptake in rat brain cortical synaptosomes in a concentration-dependent manner[4], suggesting that the effects of the venom might also involve modulation of the GABAergic system.

Compounds which increase L-glutamate uptake are of interest as the over-stimulation of glutamatergic postsynaptic receptors due to sustained elevation of extracellular L-glutamate levels in the synaptic cleft leads to excitotoxicity, which results in neuronal death through apoptosis/necrosis[5-6]. Glutamate excitotoxicity plays a key role in secondary damage following acute pathologies, including traumatic brain injury (TBI)[7-14], hyper-excitability and seizures[15-16], stroke[17-21], epilepsy[6, 16, 22-23], and cerebral and retinal ischemia[8-9, 24-29]. Excitotoxicity also produces secondary damage in chronic pathologies, including Amyotrophic lateral sclerosis (ALS)[30-31], *Alzheimer*'s disease[32], *Huntington*'s disease[33-34], neuropathic pain[35] and HIV-associated neurocognitive disorders (HAND)[36-39].

There are five structurally distinct subtypes of Na^+-dependent EAAT transporters, including (rat/human homolog): GLAST/EAAT1/, GLT-1/EAAT2, EAAC1/EAAT3, EAAT4 and EAAT5, which allows for precise spatial and temporal regulation of L-

glutamate neurotransmission[40]. Transporters EAAT1 and EAAT2, expressed predominantly in glia cells of the central nervous system, are the major transporters which take up synaptic glutamate to maintain optimal extracellular glutamic levels, thus preventing accumulation in the synaptic cleft and ensuing excitotoxicity [21, 41-44]. Although expressed within the same astrocytic plasma membrane[45], EAAT1 and EAAT2 display functional differences, for example, cell-surface protein expression of EAAT1 is affected by exogenous glutamate levels, but not EAAT2; and EAAT2 is regulated by neuronal soluble factors, unlike EAAT1[46-47]. EAAT1 is highly expressed in the glial cells of the cerebellar Purkinje cell layer [48-49] and generally is expressed at higher levels in astrocytes and oligodendrocytes compared to microglia[50]. EAAT2 is primarily expressed in astrocytes and select neurons and oligodendrocytes of the brain and spinal cord[44, 51], and accounts for approximately 95% of the total L-glutamate transport activity and 1% of total brain protein in the Central Nervous System (CNS)[27, 45, 52-54]. Growing evidence shows that dysregulation of these transporters plays a significant role in excitotoxicity and associated neuropathogenesis. The expression and function of these astrocytic transporters may be dysregulated at the genetic, epigenetic, transcriptional or translational levels, leading to high levels of extracellular glutamate and excitotoxicity[39, 55-59]. On the other hand, the neuronal EAAT3 is ubiquitously expressed in the brain, it is important in maintaining low local concentrations of glutamate, where its predominant post-synaptic localization can buffer nearby glutamate receptors and modulate excitatory neurotransmission and synaptic plasticity[60]. Several diseases implicate in dysfunction of EAAT3, such as epilepsy, Obsessive-Compulsion disorder and schizophrenia [60]. The neuronal EAAT4 and glial EAAT1 are the two predominant EAATs responsible for maintaining low extracellular glutamate levels and preventing neurotoxicity in the cerebellum, the brain

region essential for motor control, by limiting mGluR1 signalling[61]. EAAT5 is important for control of glutamate release mediates light responses in depolarizing bipolar cells in retina[62].

Termination of GABA-mediated neurotransmission is achieved by high-affinity transporters, named GATs, located at both GABAergic neurons and the surrounding astrocytes. GABA transporter subtype 1 (GAT-1, mainly presynaptic) and GABA transporter subtype 3 (GAT-3, mainly astrocytic) are the main transporters that regulate inhibitory GABAergic transmission in the mammalian brain through GABA reuptake[63]. The role of the neurotransmitter GABA in seizure disorders is not fully understood, but several studies indicate that the inhibition of GABA uptake could lead to suppression of seizures[64-66]. This is validated by studies using GABA analogues that were shown to exhibit pronounced anticonvulsant activity in a variety of animal seizure models, including tiagabine, a GAT inhibitor that has been developed as a clinically active antiepileptic drug[67]. Moreover, glycine transporters-1 and -2 (GlyT1, and GlyT2), regulate extracellular glycine concentrations within the CNS and as such, play critical roles in maintaining a balance between inhibitory and excitatory neurotransmission. The GlyT1 subtype is expressed by astrocytes at both inhibitory and excitatory synapses as well as by a subset of glutamatergic neurons, whereas the expression of GlyT2 is predominantly restricted to presynaptic terminals of inhibitory glycinergic neurons[68]. GlyT-1 inhibition has been extensively examined as a potential means to treat several CNS disorders that include schizophrenia, depression, anxiety, addiction, pain, Parkinson's disease, and epilepsy[69]. Modulation of GlyT2 transporters could provide therapeutic avenues for chronic pain, as exemplified by N-arachidonyl-glycine (NAGly), an endogenous lipid that inhibits glycine transport by GlyT2 and

shows potential as an analgesic[68], and novel allosteric modulators of GlyT2 with translational potential for pain analgesia[70].

The neuroactive properties of the venom of *P. bistriata* appeared to be related to three HPLC fractions previously isolated from the spider venom, namely Parawixin1 (Pwx1)[4, 71], Parawixin2 (Pwx2)[72-77], and Parawixin10 (Pwx10)[78-79], containing strongly polar, low molecular mass compounds.

The most polar fraction, called Pwx1, was shown to increase the rate of L-glutamate uptake *in vitro* selectively through L-glutamate transporter EAAT2. Importantly, the Pwx1 fraction also had neuroprotective properties in an *in vivo* model of glaucoma[71]. Additionally, the structural region of the transporter in which Pwx1 interacts sits at the interface of the rigid trimerization domain and of the central substrate-binding transport domain, allowing for the identification of an allosteric site that is important for transport stimulation[80]. Further studies used an *in silico* approach to screen for novel compounds that interact with this allosteric site and were shown to be positive allosteric modulators of EAAT2[81]. Importantly, additional studies revealed that this class of compounds had also *in vitro* neuroprotective properties[82], validating the premise that increasing L-glutamate clearance by activation of EAAT2 transport could serve as means of achieving neuroprotection[82].

The fraction Pwx2 inhibited the uptake of GABA and glycine in synaptosomes and exhibited anticonvulsant effects in chemically-induced seizures models in a dose-dependent manner[73-74, 77]. Furthermore, this fraction exhibited anxiolytic, neuroprotective and anti-epileptic effects in *in vivo* models of Temporal Lobe Epilepsy[72, 76]. The chemical structure of the active component in the fraction Pwx2, also called FrPbAII, was proposed as 2-amino-5-ureidopentanamide[73].

Fraction Pwx10 was shown to increase L-glutamate uptake in rat brain synaptosomes[78] and to have neuroprotective and anticonvulsant activities in *in vivo* epilepsy models of intrahippocampal *N*-methyl-D-aspartate microinjection, and pentylenetetrazole injection in the lateral ventricle[79].

With all these promising biological activities found, we decided to investigate the chemical structures of the low molecular mass components of the *P. bistriata* venom by UHPLC-HR-ESI-MS and MS/MS in an untargeted approach to get a better understanding of the complex venom composition. We were especially interested in the structure elucidation and the synthesis of the compounds that caused the observed activities in the Pwx1, Pwx2, and Pwx10 fractions in order to confirm structure and biological activity.

In this work, we have elucidated the structure of 36 acylpolyamines, with and without amino acid linkers, in the venom of the *P. bistriata* spider. One of them is the structure of (S)-N1-(3-(2-amino-5-guanidinopentanamido)propyl)-N4-(3-(2-(4-hydroxy-1H-indol-3-yl)acetamido)propyl)-N1,N1,N4,N4-tetramethylbutane-1,4-diaminium iodide (4-OH-IndAc3(Me_2)4(Me_2)3Arg^{2+}), that had equivalent biological activity to Pwx10. This compound was revealed to be a doubly charged acylpolyamine derivative showing a non-selective allosteric modulation of astrocytic L-glutamate transporters. Importantly, this compound was neuroprotective in *in vitro* models of excitotoxicity, suggesting that this class of compounds could be further developed into therapies for neurological disorders that involved L-glutamate excitotoxicity.

Results and discussion

Structure elucidation of the low molecular mass compounds in *P. bistriata* venom

The *P. bistriata* venom was extracted from the spider glands with H_2O/MeCN 9:1 (v/v) and then analyzed by UHPLC-HR-ESI-MS and MS/MS. The venom was chromatographed on a RP C_{18+} core shell column and a mobile phase composed of H_2O/MeCN + 0.1% TFA, conditions particularly suited for the separation of polar basic compounds. The MS/MS spectra were recorded in an untargeted approach with the selection of maximum five different precursor ions after one survey scan. In addition, the number of exchangeable protons of the spider venom metabolites was determined in an on-line H/D exchange experiment.

The low molecular mass compounds (< 1000 Da) in spider venom can be classified into acylpolyamine derivatives and other small molecules. The structure of these polyamine derivatives was elucidated based on the MS/MS fragmentation rules defined by *Tzouros et al.*[83]. These rules allow the unambiguous identification of acylpolyamines from their MS/MS fragment ions without the need of synthesized reference material. All polyamine derivatives were named according to the generic acylpolyamine nomenclature[84]. More details about acylpolyamine nomenclature can also be found in the supplementary material (including Figure 1 and tables 1-3). The structures of the other small compounds, which are not polyamine derivatives and, thus, do not follow the fragmentation rules of acylpolyamines, were confirmed by the analysis of reference material.

The base peak chromatogram (BPC) of a sample of crude *P. bistriata* venom measured by UHPLC-HR-MS is shown in Figure 1. With the untargeted approach, the MS and MS/MS spectra of more than 75 features were recorded. Of these, 58

structures could be resolved. The signals related to the proposed biologically active candidates found in the peak corresponding to the Pwx2 (P^+ = *m/z* 175.12)[73] and Pwx10 (*m/z* 294.72)[78] fractions were detected with a retention time of 1.13 min and 6.84 min, respectively. The molecular mass (437 Da)[4] characterizing the main compound described in the Pwx1 fraction, however, could not be related to any signal observed from the crude spider venom. Since there is no other structure-related information about the active substance in Pwx1 fraction[4] and the originally isolated fraction was no longer accessible, the structure of the active substance in Pwx1 fraction was not further investigated in this study.

Structure elucidation of the active compound in the Pwx2 fraction

Previous studies proposed 2-amino-5-ureidopentanamide (FrPbAII) as the active structure in the Pwx2 fraction[73]. In our studies, the structure of the active compound in the Pwx2 fraction was re-examined.

In the UHPLC-MS chromatogram of the crude *P. bistriata* venom, the peak related to *m/z* 175.11909 ($[M+H]^+$) was detected with a retention time of 1.13 min. Although retention time and accurate masses were in good agreement with commercially available FrPbAII (1.15 min and C6H15N4O2, $\Delta m/z$ = 0.78 ppm), the MS/MS spectra are clearly proving the presence of arginine ($\Delta m/z$ = 3.63 ppm), a structural isomer of FrPbAII (Figure 2). Our bioactivity tests with commercially available FrPbAII did not show any effect on the inhibition of GABA (Figure 3B). Additionally, the activity assays of arginine (Figure 3C) did not match to what was observed for the isolated fraction Pwx2, as none of the concentrations of arginine tested elicited inhibition of GABA uptake. This suggests that another co-eluting small molecule from the spider venom may trigger the action of Pwx2.

In total, 22 small compounds (mainly nucleosides, amino acids and quaternary amines) were identified within the venom of *P. bistriata* (see supplementary material for comprehensive data including all MS/MS spectra obtained from the spider venom as well as the corresponding reference compounds) whereby only one of the identified small compounds, namely inosine, was previously found in the *P. bistriata* venom[85]. Inosine induced convulsive seizures in rats after intracerebroventricular injection, whereas an analogue, inosine 5'-monophosphate, induced a delayed paralysis in termites[85]. In addition, adenosine and guanosine as well as the related free bases, adenine and guanine, were detected[86-89]. Nucleosides have already been found in the venom of several spider families[90-91].

In addition to arginine, which has been found in the fraction of Pwx2, the amino acids leucine, isoleucine, glutamic acid, glutamine, phenylalanine, tyrosine, and tryptophan were detected. Of all these compounds, only glutamic acid has been reported several times as component of spider venoms[91]. In insects, L-glutamate is an excitatory neurotransmitter at the neuromuscular junction[2-3]. The ion channel of the activated postsynaptic L-glutamate receptor can be inhibited by acylpolyamine compounds, which cause reversible paralysis of the spider's prey[92-94]. It seems to be quite reasonable that the L-glutamate and acylpolyamines together make the venom highly efficient. However, until now the combination of L-glutamate and acylpolyamines have only been found in venoms of spiders from the *Araneidae* family[91], in which *P. bistriata* belongs.

The venom further contains a number of quaternary amines, including choline, which was previously detected in various spider venoms[88], betaine, carnitine, acetylcarnitine, propionyl carnitine, and homarine found for the first time in the spider venom. The presence of homarine uniquely stands out since it is a compound that to

the best of our knowledge is only known from marine species. Lastly pantothenic acid as well as the polyamines spermine and spermidine were found. However, none of the three β-carboline toxins, PwTx-I[95], PwTx-II[96] and 1-guanidino-6-hydroxy-3,5-dihydro-β-carboline[97] described by the group of *Palma,* nor structural related compounds, were detected.

Activity of constituents of the fraction Pwx2

We have examined and compared the effects of the natural Pwx2 fraction with the commercially available FrPbAII on both GAT-1 and GAT-3 mediated GABA transport, as well as GlyT1 and GlyT2 mediated glycine transport. Experiments were performed in COS-7 transiently transfected with the appropriate DNA and empty vector for background. Two days after transfection, a dose response assay of Pwx2 was conducted, in presence of 50 nM of the appropriated radiolabelled isotope (figure 3). The Pwx2 fraction inhibited GABA uptake mediated by GAT-1 with an IC_{50} of 117 ± 6 μM, while it had no effect on GABA uptake mediated by GAT-3, and glycine uptake mediated by GlyT1 and GlyT2 (Figure 3A). In a previous study, natural Pwx2 fraction was shown to inhibit GABA uptake in cortical synaptosomes with an IC_{50} of 24 μg/ml, which is equivalent to 114 μM[73], a comparable value for the inhibition of GAT-1 observed herein. We also examined Pwx2 concentrations higher than 500 mM, and they did not inhibit GAT-1 mediated uptake more than ~52% (not shown in the graph for simplicity). Suggesting that the natural Pwx2 fraction, even though seemingly selective for GAT-1 rather than GAT-3 and glycine transporters, is a weak and poorly efficacious GAT-1 inhibitor, compared to other specific inhibitors, such as SKF 89976A hydrochloride (IC_{50} of 0.13 μM for GAT-1 inhibition[98]) and tiagabine, an anticonvulsant with an IC_{50} of 67 nM *in vivo*[67, 99]. Also, we did not observe any effect of the fraction

Pwx2 on glycine uptake mediated by GlyT1 or GlyT2 (figure 3), even though in the previous work it was reported to inhibit glycine uptake in synaptosomes and retinal preparations[73]. Further experiments to examine whether Pwx2 modulates other transporters, or has indirect effects on other targets, are needed to understand this discrepancy.

The commercial compound FrPbAII did not affect either GAT-1, GAT-3, GlyT1 or GlyT2 mediated GABA or glycine transport, as shown in Figure 3B, confirming that the active constituent of the Pwx2 fraction is not the originally proposed FrPbAII. The revised structure containing arginine was also tested against these 4 subtypes of transporters. However, a dose response of arginine shows that there is no effect on GAT-1, GAT-3, GlyT1 and GlyT2, suggesting that the active compound in the fraction Pwx2 is not arginine either (figure 3C). Since arginine, the main compound of the Pwx2 fraction, is not active, we speculate that the inhibiting effect of the isolated fraction Pwx2 on GAT-1 activity is either due to a minor compound or to unknown synergistic effects among different molecules within the venom. Figure 3D shows the background of GABA uptake assays obtained in presence of 1 mM nipecotic acid, resulting in inhibition of 98 ± 1.5% by GAT-1, 75 ± 4% by GAT-3. Specific GlyT1 inhibitor sarcosine results in inhibition of 90 ± 8% and specific GlyT2 inhibitor *N*-arachidonylglycine results in inhibition of 95 ± 3 %, meaning that our uptake approach was fully functional.

Other potential candidates that could be causing the effect of the Pwx2 fraction were explored, in addition to several small compounds which have been detected in the crude *P. bistriata* venom (supplementary figure 2), on GABA uptake mediated by GAT-1 and GAT-3 transporters, and glycine uptake mediated by GlyT1 transporter. Betaine, homarine, L-carnitine hydrochloride, spermidine trihydrochloride and spermine were examined, as they similar short retention times in the chromatographic

separation when the crude venom was analyzed and therefore might be part of the originally isolated fraction Pwx2. Homarine, carnitine and betaine, however, did not affect the activities of the transporters examined (supplementary figure 2A-C). On the other hand, spermidine and spermine selectivity increased the activity of GAT-1 mediated GABA uptake, without affecting the activities of GAT-3 or GlyT1 (supplementary figures 2D and E show the effects of spermidine trihydrochloride and spermine on GAT-1, respectively, with variable EC_{50s} and efficacies). Therefore, spermidine and spermine increase GAT-1 activity, an effect that seems counter-intuitive, as increased GABA transport results in less inhibitory neurotransmitter at the neuromuscular junction of insects, resulting in more excitatory inputs. However, we speculate that these effects would be annulled by the inhibiting effect of the Pwx2 fraction in GABA transport, resulting in paralysis of insects, as previously shown[1]. These findings suggest that the active constituent in the fraction Pwx2 is neither of these compounds.

Selective modulation of the GABA uptake process through pharmacological agents has been explored over several decades. These studies have demonstrated that inhibition of astroglial, but not neuronal, GATs may be preferred for anticonvulsant action. Only recently a class of specific GAT-3 inhibitors, which act by allosteric modulation, were elucidated[100]. However, it remains to be investigated whether this class of compounds has efficacy for conditions such as epilepsy in preclinical studies. So far, the only compound with notable inhibitory effects at GATs, tiagabine, has demonstrated clinical anticonvulsant efficacy, and is, to date, the only approved GAT inhibitor for clinical use. Thus, efforts to identify and develop GAT subtype-specific compounds continue to be an area of active investigation for the management of epilepsy and other CNS disorders[101].

Structure elucidation of the acylpolyamine derivatives

Earlier studies suggested that the neuroprotective effect of the fraction Pwx10 is probably due to an acylpolyamine associated with the doubly charged ion *m/z* 294.7[78]. The corresponding peak in the UHPLC-MS chromatogram of the *P. bistriata* crude venom was found at 6.84 min (Figure 1). Figure 4 displays the full scan (FS)-HR-MS spectrum related to the chromatographic peak. The molecular formula derived from the doubly charged ion *m/z* 294.72047 is $C_{30}H_{55}N_9O_3^{2+}$ (–1.00 ppm). The associated singly charged ion (*m/z* 588.4) was not detected. Instead, signals of TFA adducts at *m/z* 702.42615 ($[M^{2+}+TFA^-]^+$, $C_{32}H_{55}N_9O_5F_3^+$, –1.60 ppm), *m/z* 351.71694 ($[M^{2+}+TFA^-+H^+]^{2+}$, $C_{32}H_{56}N_9O_5F_3^{2+}$, –0.98 ppm) and *m/z* 816.41902 ($[M^{2+}+2TFA^-+H^+]^+$, $C_{34}H_{56}N_9O_7F_6^+$, –1.37 ppm) and even the signal of the triply charged ion at *m/z* 196.81624 ($[M^{2+}+H^+]^{3+}$ $C_{30}H_{56}N_9O_3^{3+}$, –0.42 ppm) were detected.

The structure of the acylpolyamine related to the main component of the Pwx10 fraction was elucidated by the MS/MS spectrum obtained from the precursor *m/z* 816.42 which was the only precursor that resulted in signals above *m/z* 231 (see supplementary material). The compound was identified as 4-OH-IndAc3(Me_2)4(Me_2)3Arg^{2+} (compound **12**; Figure 5). The base peak ion of the MS/MS spectrum *m/z* 231.11269 (a_1, $C_{13}H_{15}N_2O_2^+$, –0.49 ppm) together with the ion *m/z* 146.06007 (a', $C_9H_8NO^+$, –0.20 ppm) indicated that the acylpolyamine has a 4-hydroxy-indol acetyl head moiety connected to a C_3 amine unit. Further, the spectrum showed the fragments *m/z* 214.16636 (z_1, $C_9H_{20}N_5O^+$, 0.58 ppm), *m/z* 197.13970 (y_1, $C_9H_{17}N_4O^+$, 0.06 ppm), *m/z* 157.10854 ($C_6H_{13}N_4O^+$, 0.97 ppm), *m/z* 155.11782 (z_1-Gu, $C_8H_{15}N_2O^+$, –0.45 ppm) and *m/z* 139.09792 ($C_6H_{11}N_4^+$, 0.70 ppm), distinctive for an arginine tail linked to a C_3 unit. The identified head and tail units had to be linked

by a fragment related to the formula $C_8H_{20}N_2$. The large number of hydrogen atoms indicated that the head and tail were not simply connected by a linear C_8-unit. In fact, only a C_4-unit framed by two dimethylated nitrogen atoms matched the molecular formula of the acylpolyamine. This structure was in good agreement with the remaining major signals at *m/z* 100.11254 (dimethyl-pyrrolidin, $[C_6H_{14}N]^+$, 4.64 ppm), *m/z* 259.22392 (t_{z1}, $C_{11}H_{27}N_6O^+$, –0.64 ppm), *m/z* 313.27065 (z_2, $C_{15}H_{33}N_6O^+$, -1.23 ppm) and *m/z* 330.21728 (a_2, $C_{19}H_{28}N_3O_2^+$, –0.98 ppm).

The presence of tetrasubstituted *N*-atoms in the acylpolyamine structure was confirmed in an H/D exchange experiment. The shift from *m/z* 294.72047 ($[M]^{2+}$, $C_{30}H_{55}N_9O_3^{2+}$, –1.00 ppm) to *m/z* 299.75276 ($[d_{10}\text{-}M]^{2+}$, $C_{30}H_{45}D_{10}N_9O_3^{2+}$, 1.77 ppm) confirmed the presence of 10 exchangeable hydrogen atoms. This finding supports the proposed structure 4-OH-IndAc3(Me_2)4(Me_2)3Arg^{2+}.

The structure of 4-OH-IndAc3(Me_2)4(Me_2)3Arg^{2+} (**12**) was confirmed by the synthesis of reference material (compound **12**, see below). This acylpolyamine derivative has never been described before. However, acylpolyamines with quaternary amines in the polyamine backbone were previously reported by *Grishin et al.*[102] in *Argiope lobata, Araneidae* and by *Yamaji et al.*[103] in *Macrothele gigas*, *Hexathelidae*.

Besides the acylpolyamine related to the Pwx10 fraction, the structures of 35 additional acylpolyamines were elucidated from the venom of the spider *P. bistriata.* All elucidated structures are summarized in the matrix shown in Figure 6 and their respective backbone, tail, and head highlighted as green squares. The rows represent the head moiety and the columns a polyamine backbone of the corresponding structure (refer to supplementary material for the drawn structures and the MS/MS spectra of all the identified polyamine compounds). To our knowledge, only two of the identified acylpolyamines have been described so far. The structure of *N*-(5-

aminopentyl)-2,5-dihydroxy-benzamide (2,5-$(OH)_2$-Bz5) was reported in the venom of a *Drassodes* species (*Gnaphosidae*)[104]. N^1-5-aminopentyl)-2-[(1H-indol-3-ylacetyl)amino]-butanediamide (IndAcAsn5, Pseudoargiopinin3) was earlier found in the spider venom of *Argiope lobata*[102], a species that belongs, as *P. bistriata*, to the family of *Araneidae*.

Surprisingly, the venom of *P. bistriata* contained both types of acylpolyamines with and without amino acid linkers. They are both well known, but to the best of our knowledge they were never found coexisting in a spider venom until now. *P. bistriata* spider belongs to a more recent evolved group which also has characteristics of ancestral groups[91]. We speculate the presence of both acylpolyamines types could be related to the evolution process of this group; however, detailed studies on spider venom content attempting to correlate the phylogenetic relationships between various species of the *Araneidae* family are needed.

Acylpolyamines with the three amino acids asparagine (Asn), lysine (Lys), and arginine (Arg) in their backbone were already described by *Grishin et al.* (*A. lobata*, *Araneidae*)[102] and *Wakamiya et al.* (*Nephila species, Nephilidae)*[105-106]. They were isolated and their structures elucidated by NMR.

Somehow unusual seems the presence of the acylpolyamines N^1-(4-(2-amino-5-(dimethylamino)pentanamido)butyl)-2-(2-(2,4-dihydroxyphenyl)acetamido)succinamide (2,4-$(OH)_2$-PhAcAsn4Orn(NMe_2), see Supplementary Material p. 27), and 2-(2-(1H-indol-3-yl)acetamido)-N^1-(4-aminobutyl)pentanediamide (IndAcGln4, see Supplementary Material p. 20) as they are, so far, the only derivatives in the venom that possess an ornithine or a glutamine unit in their backbones. However, as for all other elucidated structures, the MS/MS and the determined number of exchangeable H-atoms support the proposed

structures. While glutamine was not found in a polyamine backbone before, ornithine was earlier found in nephilatoxins (*Nephila clavata*), where the presence of ornithine was confirmed by amino acid analysis[107].

Finally, the two bis-acetylated polyamine derivatives *N*,*N*'-(azanediylbis(propane-3,1-diyl))bis(2,5-dihydroxybenzamide) (2,5-$(OH)_2$-Bz33-(2,5-$(OH)_2$-Bz)) see Supplementary Material p. 23) and *N*-(3-((4-(2,5-dihydroxybenzamido)butyl)amino)propyl)-2,5-dihydroxybenzamide (2,5-$(OH)_2$-Bz34-(2,5-$(OH)_2$-Bz)), mygalin, see Supplementary Material p. 25) were detected. Their experimental data are in good agreement with the reported ESI-MS/MS spectrum of mygalin that was isolated from the hemocytes of the spider *Acanthoscurria gomesiana* (*Theraphosidae*)[108].

Synthesis of 4-OH-IndAc3(Me_2)4(Me_2)3Arg^{2+} (12)

The synthesis of 4-OH-IndAc3(Me_2)4(Me_2)3Arg^{2+} (**12**) was developed in order to unequivocally confirm the structure of the active compound in the Pwx10 fraction as compound **12** by comparison of structure and biological activity. The synthesis of the *N*-Boc protected, methoxy-indole intermediate, **10**, is shown in Scheme 1. In reaction (1) N,N-dimethylpropane-1,3-diamine (**1**) was coupled to (S,Z)-5-(2,3-bis(tert-butoxycarbonyl)guanidino)-2-((tert-butoxycarbonyl) amino) pentanoic acid (**2**) by the action of the coupling reagent T3P to provide the key N,N-dimethylpropane tri-N-Boc protected arginine amide (**3**), which will become the right hand side motif of 4-OH-IndAc3(Me_2)4(Me_2)3Arg^{2+} (**12**). In reaction (2) 4-methoxy-1H-indole, **4**, was reacted with oxalyl chloride followed by quenching with methanol to produce methyl 2-(4-methoxy-1H-indol-3-yl)-2-oxoacetate, **5**. The reactive carbonyl in **5** is reductively removed under palladium hydrogenation conditions to yield methyl 2-(4-methoxy-1H-

indol-3-yl)acetate, **6**, which is then hydrolysed to provide 2-(4-methoxy-1H-indol-3-yl)acetic acid, **7**. Compound **7** is then used to build the left-hand side motif of 4-OH-IndAc3(Me_2)4(Me_2)3Arg^{2+} (**12**), first by amide coupling with diamine **1**, by the action of T3P in Hunigs base and dichloromethane, followed by alkylation with 1,4-diiodobutane to provide 4-iodo-N-(3-(2-(4-methoxy-1H-indol-3-yl)acetamido)propyl)-N,N-dimethylbutan-1-aminium iodide, **9**. Alkylation of **9** by the N,N-dimethyl amine of intermediate **3** shown in reaction (4) provides the protected precursor, (S,Z)-N1-(6,11-bis((tert-butoxycarbonyl)amino)-2,2-dimethyl-4,12-dioxo-3-oxa-5,7,13-triazahexadec-5-en-16-yl)-N4-(3-(2-(4-methoxy-1H-indol-3-yl)acetamido)propyl)-N1,N1,N4,N4-tetramethylbutane-1,4-diaminium iodide, **10**.

Scheme 2 shows the first approach at a stepwise removal of the protecting groups by first removing the *N*-Boc protecting groups in reaction (5) by the action of trifluoroacetic acid in dichloromethane to provide the methoxyindole **11**. However, due to the polarity of **11**, we were unsuccessful in being able to further remove the indole methoxy group for this compound. Therefore, as shown in reaction (6) **10** was treated with boron tribromide at -78 ^{o}C to remove the indole methoxy group under mild conditions. Then by allowing the reaction mixture to slowly warm to room temperature the reaction mixture became acidic enough to remove the *N*-Boc protection to provide 4-OH-IndAc3(Me_2)4(Me_2)3Arg^{2+} (**12**), in a 45% yield after reverse phase HPLC purification. Please see supplementary material for NMR and MS spectra for all compounds.

Compound **12** was then fully characterized for comparison against the isolated compound from the spider venom, and further evaluated for biological activity in neurotransmitter transport and neuroprotection assays, as described below.

Effects of Pwx10 fraction, and compounds 11 and 12 on neurotransmitter transporter studies

Our results indicate that the natural Pwx10 fraction stimulated L-glutamate uptake through EAAT1 and EAAT2 with no effects on EAAT3-mediated uptake. Figure 7A shows dose response curves for the effect of the Pwx10 fraction, with the potencies and efficacies are expressed as mean ± SD of three independent experiments. The compound was found to have similar potencies for EAAT1 and EAAT2- mediated L-glutamate uptake, with EC_{50} of 5.8 ± 2.9 nM for EAAT1 and 5.2 ± 2.4 nM for EAAT2. Efficacies of uptake augmentation were also similar, with 162 ± 11% for EAAT1 and 168 ± 9 for EAAT2. To validate the effect of natural Pwx10 fraction in an endogenous system, we performed dose response assays for the Pwx10 fraction in cultured glia (Figure 7B), and demonstrated that the compound has a potency of 22 ± 7 nM and efficacy of 314 ± 16% for L-glutamate uptake augmentation.

L-glutamate uptake kinetic analysis of the effect of different concentrations of the Pwx10 fraction (10, 100 and 500 nM) in EAAT1 and EAAT2 transfected cells, respectively, are shown in Figure 7C and D. For EAAT1-mediated uptake, V_{max} values were significantly increased, from 127 ± 15 pmol/well/min for control (vehicle) conditions, to 168 ± 7, 313 ± 33 and 783 ± 23 pmol/well/min in presence of increasing concentrations of the Pwx10 fraction. K_m values were not significantly different among conditions. For EAAT2-mediated uptake, V_{max} values were significantly increased, from 133 ± 14 pmol/well/min for control (vehicle) conditions, to 170 ± 9, 309 ± 19 and 797 ± 26 pmol/well/min in presence of increasing concentrations of the Pwx10 fraction. K_m values were not significantly different among conditions. These results that the active compound in the Pwx10 fraction acts as a non-selective enhancer of the activity of both subtypes of astrocytic L-glutamate transporters EAAT1 and EAAT2. Since the

affinity for the substrate (K_m) values were not significantly different among conditions (One-way ANOVA followed by Dunnett's *post-hoc* test comparing to vehicle), with an average ± SD of 53 ± 4 μM for EAAT1 and 52 ± 6 μM for EAAT2, we propose that the mechanism of stimulation to be through positive allosteric modulation of the transporters. Figure 7E shows a kinetic experiment performed in cultured glia in presence of different concentrations of the Pwx10 fraction, showing that the V_{max} values were significantly increased, from 19.7 ± 1 pmol/well/min for control (vehicle) conditions, to 38.2 ± 1.3 and 59.4 ± 3.3 pmol/well/min in presence of 100 and 500 nM Pwx10 fraction. Similarly to the results in transfected cells, the K_m values were not significantly different among conditions (One-way ANOVA followed by Dunnett's *post-hoc* test comparing to vehicle), with an average ± SD of 44 ± 3 μM, suggesting once again that the active compound in the Pwx10 fraction might be an allosteric modulator of the activity of the transporters.

We proceed with our studies to examine the actions of synthesized compounds **11** and **12** (shown in Scheme 2). Compound **12** corresponds to the structure of the potential active substance in the isolated Pwx10 fraction and compound **11** is a structural analogue that has a methoxy group on the left-hand side indole ring instead of a hydroxyl group. Dose response curves for the effects of **12** and **11** in transfected COS-7 cells are shown in Figure 8A and B, respectively. Acylpolyamine **12** increases EAAT1-mediated L-glutamate uptake with an EC_{50} of 0.4 ± 0.2 nM and efficacy of 171 ± 15%, and for EAAT2-mediated uptake with an EC_{50} of 0.8 ± 0.1 nM and potency of 144 ± 7%, with no effect on EAAT3-mediated L-glutamate uptake. Figure 8C shows dose response assays for **12** and **11** in cultured glia, demonstrating that the compounds increase L-glutamate uptake in this approach, however, the potency of **12** is higher (EC_{50} of 21 ± 0.6 nM) as compared to **11** (EC_{50} of 690 ± 50 nM), whereas

efficacies for augmentation were similar (178 ± 9% for **12** and 155 ± 9% for **11**), indicating that the methoxy group in **11** results in lower potency for L-glutamate augmentation.

Kinetic analysis of L-glutamate uptake in presence of different concentrations of **12** and **11** are shown in Figures 8D-F. For EAAT1-mediated uptake (figure 8D), V_{max} values were significantly increased, from 185 ± 15 pmol/well/min for control (vehicle) conditions, to 303 ± 26 and 723 ± 44 pmol/well/min in presence of 100 and 500 nM of **12**, and to 241 ± 22 and 475 ± 27 pmol/well/min in presence of 100 and 500 nM of **11**. For EAAT2-mediated uptake (Figure 8E), V_{max} values were significantly increased, from 127 ± 12 pmol/well/min for control (vehicle) conditions, to 262 ± 22 and 613 ± 55 in presence of 100 and 500 nM **12**, and to 271 ± 19 and 586 ± 22 pmol/well/min in presence of 100 and 500 nM **11**, respectively. K_m values were not significantly different among conditions (One-way ANOVA followed by Dunnett's *post-hoc* test comparing to vehicle), with an average ± SD of 62 ± 22 μM for EAAT1 and 57 ± 7 μM for EAAT2. These results demonstrate that **12** and **11** act as a non-selective enhancer of the activity of both subtypes of astrocytic L-glutamate transporters EAAT1 and EAAT2, with potentially an allosteric mechanism, since the affinity for the substrate (Km) value was not different. Figure 8F shows kinetic experiments performed in cultured glia showing that the V_{max} values were significantly increased, from 18.1 ± 1 pmol/well/min for control (vehicle) conditions, to 33 ± 2 and 55 ± 2 pmol/well/min in presence of 100 and 500 nM **12** and 28 ±1 and 37 ±2 pmol/well/min in presence of 100 and 500 nM **11**. Similarly to the results in transfected cells, the K_m values were not significantly different among conditions (One-way ANOVA followed by Dunnett's *post-hoc* test comparing to vehicle), suggesting once again that these compounds enhance the

glutamate translocation rate, with no effect on substrate interaction, suggesting an allosteric mechanism.

Collectively, results in Figure 8 indicate that the bioactivity of synthetic compounds **12** and **11** match the activity of the natural Pwx10 fraction, with **11** being slightly less potent in cultured glia cells. This data suggests that the 4-methoxy substituent on the indole ring of **11** does not negatively impact the biological activity of this component and inspires the synthesis of additional substituted indole analogs in the future to elaborate on the structure activity relationships for this motif. Notably other polyamine spider toxins containing a 4-hydroxy-indole acetic acid moiety, such as in **12**, are found to be less toxic than those with a hydroxyphenyl-based aromatic head group[109]. With these results of the activity study and the confirmation that the structure of compound **12** corresponds to the acylpolyamine in the *P. bistriata* venom, we conclude that the acylpolyamine 4-OH-IndAc3(Me_2)4(Me_2)3Arg^{2+} (**12**) is the active compound in the fraction Pwx10.

Neither the natural Pwx10 fraction nor the synthetic compounds **12** and **11** have any effect on GABA uptake mediated by GAT-1 and GAT-3, glycine uptake mediated by GlyT1 and GlyT2, and on monoamine transporters (human serotonin (hSERT), noradrenaline (hNET) and dopamine (hDAT), demonstrating these compounds are selective for L-glutamate transporters (supplementary Figure 3).

Previous studies of the three-dimensional structure of the EAAT reveal that the transporter is divided into two domains: a transport domain containing the substrate binding sites, and surrounding it a peripheral rigid scaffold, designated the trimerization domain[110-111]. The trimerization domain provides the interaction interface between the three subunits of the trimer and is believed to facilitate the elevator-like movement of the inner transport domain[112-113]. Our previous work suggests that

residues at the interface between the transport and the trimerization domains are critical for transport stimulation[80]. Intriguingly, preliminary modeling analysis of the three-dimensional structure of the EAAT, searching for residues that are similar in EAAT1 and EAAT2 (but different in EAAT3), revealed multiple molecular determinants that could be involved in the interaction of compound **12** with transporters EAAT1 and EAAT2 (not shown). Therefore, at this point, we are unable to propose a mechanism of interaction between compound **12** and EAATs. However, we speculate that the compound might be binding to the similar previously identified allosteric site[80], and possibly accelerating the rate of the transport by facilitating the movement of the transport domain, like the recently identified positive allosteric modulators (PAMs) of EAAT2[81-82]. Therefore, future studies including additional molecular modeling and mutagenesis of key residues are needed to investigate mechanisms of interaction of 4-OH-IndAc3(Me_2)4(Me_2)3Arg^{2+} (**12**) with the glial transporters.

Regrettably, other PAMs and negative allosteric modulators (NAMs) of transporters with similar structures of **12** are not available to date. However, several allosteric modulators of glutamate receptors, such as AMPA, NMDA and metabotropic glutamate receptors, have been identified[114]. For instance, polyamines spermine and spermidine act as PAMs of the NMDA receptor to potentiate channel activity. It is thought that they act by binding to the amino-terminal domain, resulting in the separation of the GluN1R and GluN2R domains and opening of the ion channel[114]. Due to remarkably different functions and mechanisms between these receptors and the EAATs, we refrain to suggest any mechanistic similarities of these PAMs and compound **12.** However, polyamines from spider venoms have been studied for a long time, and it is well stablished that many of them act as ionotropic glutamate receptor antagonists of the vertebrate and invertebrate central nervous systems[115]. Some

examples include the polyamine toxins Joro spider toxin-3 (JSTX-3) and Nephila polyamine toxins-1 and -8 (NPTX-1 and NPTX-8), isolated from the venom of the orb-weaver spider *Nephila clavata* (Joro spider). These are very potent open-channel blockers of ionotropic glutamate receptors, providing pharmacological tools for studies of these receptors[116]. Likewise, compounds **11** and **12** could be used in the future as pharmacological tools to study the molecular scaffolds in the glial transporters that they modulate.

Effects of Pwx10 fraction and compound 12 on excitotoxic insults in mixed neuron-glia cultures

We evaluated Pwx10 fraction and the acylpolyamine 4-OH-IndAc3(Me_2)4(Me_2)3Arg^{2+} (**12**) for neuroprotective effects after prolonged (24 h) excitotoxic insults with application of L-glutamate or acute (20 min) insults with oxygen-glucose deprivation (OGD), in mixed neuron-glia cultures. Our cultures had optimized growth conditions to result in ~15% of glia growth in the cultures after 14 DIV[82]. As positive control for neuroprotection, we used APV (DL-2-Amino-5-phosphonopentanoic acid), an NMDA receptor blocker. We examined the neuroprotective potential of these compounds by immunocytochemical analysis, comparing MAP-2 expression among different experimental groups, as previously described[82].

Neuronal survival after L-glutamate insult and treatments with Pwx10 fraction and compound 12

Cultures were grown for 14 DIV before treatments, then subjected to 24h insult in presence of vehicle (control), or natural Pwx10 fraction or synthetic compound **12**.

Figure 9A show representative images of cultures on different conditions. At baseline conditions (no L-glutamate insult or compound treatment - vehicle), neurons did not display pyknotic nuclei or neurite damage, which are indicators of neuronal death[117-118]. Neurons treated with Pwx10 fraction alone (100 μM; 24 h) also resemble the baseline vehicle conditions, suggesting that the components in the Pwx10 fraction are not neurotoxic. After L-glutamate insult, we observed reduced MAP-2 staining and DAPI positive, MAP-2 negative cells, indicators of cell death. On the other hand, neurons subjected to acute L-glutamate insult in presence of Pwx10 fraction (100 nM; 24 h) displayed morphological characteristics similar to baseline vehicle conditions, suggesting that this compound is neuroprotective in an excitotoxic environment.

Total neuronal survival levels from different experimental conditions were quantified. Figure 9 B illustrates the neuroprotective effects of both Pwx10 fraction and compound **12**, following the application of 100 μM L-glutamate insult in 14 DIV mixed neuron-glia cultures. Application of 100 μM L-glutamate significantly decreased neuronal survival to 25.9 ± 15.4% of baseline vehicle levels (red bar). Only application of 100 nM Pwx10 fraction or **12** after L-glutamate insult resulted in a significant neuroprotective effect, increasing survival levels to 70.5 ± 13.4 (Pwx10 fraction) and 64.4 ± 0.5% (**12**) of baseline whereas 1 nM and 10 nM of the Pwx10 fraction did not increase neuronal survival compared to the insult condition. To determine if the neuroprotective effect of 4-OH-IndAc3(Me_2)4(Me_2)3Arg^{2+} requires an active L-glutamate transporter, we subjected mixed cultures to prolonged L-glutamate insult, followed by co-treatment with 100 nM Pwx10 fraction and the L-glutamate transport inhibitor TBOA (100 μM), that inhibits all transporter subtypes at this concentration, and with the selective EAAT2 inhibitor WAY 213613 (1 μM). Co-treatment of 100nM of Pwx10 fraction with both L-glutamate transport blocker TBOA and EAAT2 specific

inhibitor WAY 213613 abolish the neuroprotective effect of the compound. Co-treatment with TBOA results in a more significant knockdown of the neuroprotective effects of Pwx10 fraction compared to co-treatment with WAY 213613, which is consistent with our findings that the Pwx10 fraction increases L-glutamate uptake through both EAAT1 and EAAT2. Finally, treatment with positive control APV results in significant neuroprotection, with survival at 80.7 ± 2.7% of baseline, confirming the viability of our cultures, and suggesting that excessive L-glutamate transmission through the NMDA receptor plays a crucial role in L-glutamate excitotoxicity and neuronal death[119-120], thus providing a positive control to measure the effect of the active compound in the Pwx10 fraction.

To better understand the contribution of the different subtypes of EAATs in the mixed neuron-glia system, L-glutamate uptake assays in presence of several inhibitors were performed. Supplementary Figure 3 indicates that L-glutamate uptake in presence of 1 μM WAY 213613 inhibits 50 ± 5% of L-glutamate uptake. At this concentration, this inhibitor is selective for EAAT2 inhibition over EAAT1 and EAAT3, indicating that ~ 50% of the transporters in this approach are EAAT2. On the other hand, UCPH-101, at 1 μM, a concentration that displays a selective inhibition of EAAT1 over the other subtypes, inhibits 23 ± 8% of L-glutamate uptake, suggesting that ~25% of the transporters in this system are comprised of EAAT1. When co-incubated with both inhibitors, the transport is inhibited to a level of 6.5 ± 0.5%, indicating the L-glutamate uptake in these cultures is mediated by EAAT1 and EAAT2, with a small percentage of uptake probably due to EAAT3.

Neuronal survival after Oxygen Glucose Deprivation (OGD) insult and Pwx10 fraction and compound 12 treatments

In these studies, we also evaluate Pwx10 and 4-OH-IndAc3(Me_2)4(Me_2)3Arg^{2+} (**12**) in an *in vitro* stroke model, by subjecting the cultures to OGD insults. Figure 10 A shows representative images of vehicle (control) cultures, under OGD conditions, and under OGD followed by treatment with 100 nM Pwx10 fraction. As seen above, vehicle (control) cultures do not display pyknotic nuclei or neurite damage, as opposed to OGD-treated cultures, in which there is a reduction in MAP-2 staining and DAPI positive, MAP-2 negative cells, indicators of cell death. On the other hand, neurons subjected to OGD insult followed by incubation of Pwx10 fraction (100 nM; 24 h) displayed morphological characteristics like baseline vehicle conditions, suggesting that this compound is neuroprotective in an excitotoxic environment. The quantification, showed in Figure 10 B, illustrates that the Pwx10 fraction and compound **12** displayed neuroprotective effects following 20 minutes of OGD. Application of 10nM and 100 nM Pwx10 fraction and acylpolyamine **12** following the OGD insult significantly increasing neuronal survival from 29.5 ± 9.6% of baseline to 70.4 ± 9.6% and 78.7 ± 4.2%, respectively. Intriguingly, the concentration of 10 nM Pwx10 fraction was able to confer neuroprotection in this OGD model, unlike following L-glutamate insults, where only 100 nM was effective. Future experiments determining extracellular concentration of L-glutamate in both models could help examine the discrepancy in effectiveness between the models. Pwx10 fraction at 1nM does not display significant neuroprotective effects, only increasing neuronal survival to 49.7 ± 21.6% compared to the control condition. Synthetic compound **12** at 100 nM displays similar neuroprotective effects compared to the natural compound, increasing neuronal survival to 89.3 ± 23.9%. Co-administration with TBOA and WAY 213613

both result in no increases in neuronal survival, and this indicates again that the neuroprotective effects of 4-OH-IndAc3(Me_2)4(Me_2)3Arg^{2+} (**12**) from OGD-induced injury is due to modulation of L-glutamate transporters.

Previous studies evidence that L-glutamate excitotoxicity plays an essential role in the neurodegeneration observed following ischemic stroke and key elements involved in excitotoxicity[121], like L-glutamate transport, may serve as potential targets for neuroprotection after ischemic stroke. In this study, we have shown that 4-OH-IndAc3(Me_2)4(Me_2)3Arg^{2+} (**12**) was neuroprotective in this model of *in vitro* insult. It is important to note that under ischemic conditions, an increase in extracellular L-glutamate can happen by reversal of uptake[122-123]. However, upon cessation of the insult, it has been shown that L-glutamate transport activity recovers[124]. We speculate that 4-OH-IndAc3(Me_2)4(Me_2)3Arg^{2+} (**12**) is still able to accelerate the removal of L-glutamate to restore homeostasis during the 24h recovery time period following the insult. This concept is supported by previous work with EAAT2 expression enhancers, including ceftriaxone and riluzole, that offer significant protection of neuron tissues against ischemic excitotoxicity[19, 125-128]. In future studies, we plan to determine the L-glutamate concentration in culture media after insult and compound treatments to complement and strengthen the notion that the mechanism of 4-OH-IndAc3(Me_2)4(Me_2)3Arg^{2+} (**12**) is through increased EAAT1/EAAT2 activity resulting in increased L-glutamate clearance. Additionally, future studies will determine whether NMDA, AMPA and kainate glutamate receptors modulation is involved, as inhibition of these could result in neuroprotection (as seen in our assays with APV, an NMDA receptor blocker). We will also examine whether metabotropic L-glutamate receptors modulation is involved in the action of compound **12** on transporters, as these receptors can exert different actions (toxic or compensatory) in response to excitotoxic

stimuli[129]. Future studies will also investigate whether apoptosis is occurring, and which intracellular signalling pathways are involved in the insult models.

Conclusions

In this work, we attempted to elucidate the chemical structures of compounds with intriguing and promising biological activities that are part of three HPLC fractions that were collected from the venom of *P. bistriata* spiders, namely Pwx1, Pwx2 and Pwx10. Furthermore, we have shown that the *P. bistriata* venom contains 36 acylpolyamines with and without amino acid linkers in their structures, a unique finding as both types of substances were never found coexisting in a spider venom until now. In addition, the presence of nucleosides and other small compounds such as amino acids free polyamines and quaternary amines was shown. Regrettably, our approach did not yield the identification of the chemical structure of the active substance in the Pwx1 fraction. Nonetheless, previous studies used this fraction to identify the region of L-glutamate transporter EAAT2 responsible for transport stimulation[80]. This important knowledge was used to identify novel compounds that were shown to be positive allosteric modulators of EAAT2[81]. We speculate that one or several unknown minor active components, have, at least in part, a similar structure of these allosteric modulators. We consider that the identification of novel positive allosteric modulators (PAMs) of EAAT2 holds promise to further drug development and to further our understanding of allosteric modulation of L-glutamate transporters.

Regarding the compound found at *m/z* 175.2 in the Pwx2 fraction, we could not confirm the presence of the previously proposed structure 2-amino-5-ureidopentanamide (FrPbAII) in *P. bistriata* venom, but the amino acid arginine. Unfortunately, neither arginine nor any of the additional constituents (betaine,

homarine, L-carnitine hydrochloride, spermidine, or spermine) acted like the Pwx2 fraction, which is as a weak inhibitor of GABA uptake through selective modulation of GAT-1. We speculate that this activity is either due to an unknown minor component of the fraction or to unknown synergistic effects among different molecules within the venom.

Regarding the Pwx10 fraction, we successfully identified its major component to be an acylpolyamine with the chemical structure 4-OH-IndAc3(Me_2)4(Me_2)3Arg^{2+} (**12**). Subsequently, compound **12** and analogue **11** were synthesized and we further confirmed their biological activity in neurotransmitter uptake assays.

Additionally, the compounds displayed neuroprotective properties after *in vitro* excitotoxic insults, an effect that was abolished in presence of L-glutamate transport inhibitors, suggesting dependence of active L-glutamate transporters. Strikingly, since mixed neuron-glia culture approach we used has ~15% of glia[82], we speculate that the neuroprotective effects of this class of compounds *in vivo*, where the proportion of glia to neurons is at least 1:1 and has been suggested to be as high as 10:1 [130], would be amplified. Indeed, previous studies revealed the Pwx10 fraction to be neuroprotective after intracerebral ventricular administration in two *in vivo* epilepsy models[78-79]. When considering potential future translational studies, it is worth noting the activity of compound **12** on EAAT1 and EAAT2 is desirable, as targeting astrocytic glutamate transporters over neuronal transporters may be beneficial over activation of neuronal transporters, such as EAAT3 and EAAT4. After clearance into astrocytes by EAAT1 and EAAT2, glutamate is converted to glutamine, which is exported to neurons and re-converted to glutamate[131], contributing to the glutamate-glutamine cycle pathway for recycling of neurotransmitter pools of glutamate[58, 132]. Furthermore, allosteric modulation is likely better suited to maintaining the highly precise temporal and spatial

aspects of glutamatergic synaptic transmission[114]. On the other hand, neuronal transporters EAAT3 and EAAT4 are localized to the postsynaptic neuron near NMDA, AMPA, and kainate receptors and metabotropic glutamate receptors (mGluR), such as mGluR5, and their modulation could lead to receptor activation and may have unwanted liabilities as a consequence of downstream signaling [133-134].

However, we have not studied this compound for its pharmacokinetic exposure *in vivo* either in plasma or in the CNS. Polycationic compounds may be toxic due to their propensity to accumulate in tissue or in mitochondria. Due to the peptidic nature of the compound, it is predicted to be metabolically unstable *in vivo*, although this needs to be confirmed. Additionally, synthesizing the compound on scale would require significant efforts, since it involves a multistep synthesis and the resulting highly polar product required HPLC purification (Schemes 1 and 2). Hence, compound **12** seems to be a good tool compound for proof of concept studies, as drug development progression studies are unlikely.

It is well known that L-glutamate excitotoxicity is implicated in a wide range of CNS disorders, such as TBI, epilepsy and chronic neurodegenerative diseases. Safe and effective pharmacological approaches to treat patients after excitotoxic events are urgently needed. This study offered proof of concept of the neuroprotective properties of 4-OH-IndAc3(Me_2)4(Me_2)3Arg^{2+} (**12**). We conclude that acylpolyamines, as well previously identified EAAT2 PAM compounds, provide a starting point for identification of a new class of neuroprotective compounds that function by enhancing the removal of excessive L-glutamate in the synaptic cleft and preventing L-glutamate-mediated excitotoxicity.

Materials and Methods

Chemicals

UHPLC grade H_2O (< 5ppb) was obtained by purification of deionized H_2O with a *MilliQ* gradient apparatus (Millipore, Milford, MA, USA). Acetonitrile (MeCN) was obtained from Fluka (LC-MS grade, Buchs, Switzerland) and trifluoroacetic acid (TFA) from Biosolve (Valkenswaard, Netherland). The reference chemicals were purchased from the companies as indicated: *L*-isoleucine, *L*-leucine, *L*-phenylalanine, spermine hydrochloride, spermidine, serotonin hydrochloride and *D*-pantothenic acid Calcium salt (Fluka, Buchs, Switzerland), *L*-tryptophan (Merck, Darmstadt, Germany), *D*-tyrosine (Novabiochem Merck, Darmstadt, Germany), betaine (Acros Chemie Brunschwig, Switzerland), adenosine, guanosine, inosine, *L*-carnitine hydrochloride, O-acetyl-*L*-carnitine and propionyl-*L*-carnitine (Sigma-Aldrich, Buchs, Switzerland). Commercial FrPbAII was purchased from Enzo Life Sciences (Farmingdale, NY, USA).

Homarine was synthesized according to literature[135]. The chemicals used for synthesis, methyl iodide, 2-pyridinecarboxylic acid, propylene oxide, diethyl ether and methanol, were obtained from Sigma-Aldrich (Buchs, Switzerland).

Natural Pwx2 fraction was isolated from the venom of *P. bistriata* spider according to previous methodology[73]. Natural Pwx10 fraction was purified as described by [76].

Non-radiolabelled *L*-glutamate and compounds arginine and nipecotic acid were purchased from Millipore-Sigma (Billerica, MA, USA). Compounds (2R)-amino-5-phosphonovaleric acid (APV), DL-threo-β-Benzyloxyaspartic acid (DL-TBOA), WAY 213613, sarcosine and N-Arachidonylglycine were purchased from Tocris (Bristol, United Kingdom).

Transfection reagent TransIT-LT1 was from Mirus Bio LLC (Madison, WI, USA).

Radiolabelled substrates, [^{3}H]-glutamic acid (51.1 Ci/mmol), [^{3}H]-glycine (48.7 Ci/mmol), [^{3}H]-GABA (92.1 Ci/mmol), [^{3}H]-dopamine (53.6 Ci/mmol), [^{3}H]-serotonin (28.2 Ci/mmol), [^{3}H]-norepinephrine (14.9 Ci/mmol), were purchased from Perkin Elmer (Boston, MA, USA).

For cell lines, culture media, including Dulbecco's modified Eagle's medium (DMEM) with glucose, fetal bovine serum, penicillin/streptomycin and blasticidin were obtained from Thermo Fisher Scientific (Waltham, MA, USA).

Scintillation fluid was obtained from Thermo Fisher Scientific (Waltham, MA, USA).

For primary cultures, cell culture media including Neurobasal medium with pyruvate, glucose-free Dulbecco's Modified Eagle Medium (DMEM, OGD media), glutamine, gentamicin, HEPES (1 M), B27, Poly-L-lysine and DNase were purchased from Sigma-Aldrich (St. Louis, MO, USA). Neurobasal-A, glutamine and B-27 supplement were obtained from Thermo Fisher Scientific (Waltham, MA, USA). Fetal bovine serum and horse serum were purchase from Hyclone (South Logan, UT, USA).

Poly-lysine coated 96-well plates and phosphate-buffered saline (D-PBS) were purchased from Corning (Corning, NY, USA).

Tools for animal dissection was purchased from Biomedical Research Instruments (Silver Spring, MD, USA).

General Chemistry

All reactions were conducted under an inert gas atmosphere (nitrogen or argon) using a Teflon-coated magnetic stir bar at the temperature indicated. Commercial reagents and anhydrous solvents were used without further purification. Removal of solvents was conducted by using a rotary evaporator, and residual solvent was removed from nonvolatile compounds using a vacuum manifold maintained at approximately 1 Torr.

All yields reported are isolated yields. Preparative reversed-phase high pressure liquid chromatography (RP-HPLC) was performed using a Gilson GX-271 semi-prep HPLC, eluting with a binary solvent system A and B using a gradient elusion (A, H_2O with 0.1% trifluoroacetic acid (TFA); B, CH_3CN with 0.1% TFA) with UV detection at 220 nm. Low-resolution mass spectral (MS) data were determined on an Water Acquity QDa LCMS mass spectrometer with UV detection at 254 nm. ^1H NMR spectra were obtained on a Bruker Avance II 400 (400 MHz) spectrometer. Chemical shifts (δ) are reported in parts per million (ppm) relative to residual undeuterated solvent as an internal reference. The following abbreviations were used to explain the multiplicities: s = single; d = doublet, t = triplet, q = quartet, dd = doublet of doublets, dt = doublet of triplets, m = multiplet, br = broad.

Spider collection and preparation of the venom extract

The *P. bistriata* spiders were collected according to the Brazilian Chico Mendes Institute for the Biodiversity Conservation (ICMBio- SISBIO protocol No. 46797) by the group of *Ferreira dos Santos* at Ponta Grossa (Paraná state, Brazil) and Marília, (São Paulo state, Brazil) and stored in dry ice. The species was identified by *Professor W. Ferreira dos Santos*. The crude venom glands from *P. bistriata* spiders were extracted in H_2O/MeCN 9:1 (gland/solvent 1:5 [m/v]), centrifuged (10,621× g; 10 min; 4 °C) and the supernatant was lyophilized, and weighed. To remove large proteins, the venom extract was again dissolved in H_2O/MeCN 9:1 and filtered *(Amicon Ultra – 0.5mL Centrifugal Filters 3,000 NMWL (Millipore,* Milford, MA, USA), 14,000 rpm, 4 °C). The filtered solution was lyophilized. For UHPLC analysis the venom was dissolved in H_2O/MeCN 9:1 + 0.05 % TFA at 10 μg μl^{-1}. All reference compounds were dissolved in H_2O/MeCN 9:1 at 10 μg ml^{-1}. The samples were stored at -20 °C prior to use.

UHPLC-MS and MS/MS

The UHPLC separations were performed on a *Dionex UltiMate 3000* HPLC instrument (*Thermo Scientific*, Germering, Germany) equipped with an autosampler, a pump and a diode-array detector (DAD) of the same producer series. The samples were chromatographed at a flow rate of 0.30 ml min^{-1} on a RP-C_{18+} column (*Cortecs™ UPLC*® C_{18+} 1.6 µm, 2.1x150 mm, *Waters*, Milford, MA, USA) with solvents A and B consisting of H_2O + 0.05% TFA and MeCN/H_2O 8:2 [*v/v*] + 0.05% TFA, respectively. The column chamber temperature was set to 25 °C. The samples were injected at a volume of 1 µl. The strong wash was MeOH and weak wash H_2O/MeCN 95:5 [v/v]. The gradient went from 3.8 to 25% of eluent B over 22 min. Finally, the column was regenerated at 100% B for 4 min and equilibrated at 3.8% B over 6 min.

The UHPLC system was connected to a *QExactive Orbitrap* FT high-resolution mass spectrometer (*Thermo Scientific*, Waltham, MA, USA) equipped with an HESI source. The MS conditions were: sheath gas flow rate (N_2, 48), aux gas flow rate (N_2, 11), aux gas heater temperature (320 °C) and sweep gas flow rate (N_2, 2), spray voltage (3.5 kV), S-lens RF level (55), capillary temperature (256 °C). Full scan MS were performed in positive ion mode at 70'000 resolutions and was between *m/z* 100 to 1500. The AGC target setting for full scan MS experiment was set to 10^6 with a maximum of 30 injection times. The mass spectrometer was calibrated for mass accuracy once a day according to the manufacturer's instructions. The relative mass error being typically lower than 2 ppm (externally).

The MS/MS experiments were acquired in Full MS/$ddMS^2$ (Top N) mode with a maximum of five ions to trigger after one survey scan. The resolving power was set to 17'500. The acquisition was performed with an isolation window set to 0.8 *m/z*. The

AGC target setting was set to 10^5. The normalized collision energy (NCE) was set to a gradient (30, 35, 40). The MS/MS spectra were recorded of the top five ions.

H/D exchange experiment

On-line H/D exchange was done on the same instrumental set up. For the chromatography, the solvents A and B consisted of D_2O + 0.05% d_1-TFA and MeCN/D_2O 8:2 [v/v] + 0.05% d_1-TFA, respectively. The column chamber temperature was set to 40 °C. The chromatogram was recorded in FS-MS mode only (no MS/MS data recorded). All other parameters remained the same.

Synthesis of 4-OH-IndAc3(Me_2)4(Me_2)3Arg^{2+} (12)

Schemes 1-2 show the synthesis of 4-OH-IndAc3(Me_2)4(Me_2)3Arg^{2+} (**12**).

(S, Z)-Tert-butyl 2, 17, 17-trimethyl-7,15-dioxo-16-oxa-2, 6, 12, 14-tetraazaoctadecan-8-yl-13-ylidenedicarbamate (3):

N1,N1-dimethylpropane-1,3-diamine (**1**) (129 mg, 1.26 mmol) and (Z)-5-(2,3-bis(tert-butoxycarbonyl)guanidino)-2-(tert-butoxycarbonylamino) pentanoic acid (**2**) (500 mg, 1.05 mmol) were combined in 20 mL of dry CH_2Cl_2 at 0 °C with stirring. Then diisopropylethylamine (0.75 mL, 4.18 mmol) was added followed by the dropwise addition of 50% solution of T3P in CH_2Cl_2 (871 mg, 1.37 mmol). The reaction mixture was then stirred for 1h at 0 °C. Completion of the reaction was confirmed by LC-MS, then the reaction mixture was quenched with water and the product was extracted with CH_2Cl_2 and dried over anhydrous Na_2SO_4. After filtration the solvent was evaporated under reduced pressure to obtain the crude product residue which was purified by silica gel flash column chromatography to afford the title compound **3** (496 mg, 84%) as a white solid. The product was confirmed by ^1H NMR & MS.

^{1}H NMR (400 MHz, $CDCl_3$): δ 11.46 (1H, s), 8.36 (1H, t, J=4.9 Hz), 7.53 (1H, s), 5.40 (1H, d, J=7.2 Hz), 4.18-4.02 (1H, m), 3.54-3.26 (4H, m), 2.49-2.38 (2H, m), 2.28 (6H, s), 1.92-1.78 (1H, m), 1.74-1.57 (5H, m), 1.498 (9H, s), 1.490 (9H, s), 1.44 (9H, S). MS: *m/z* 581 ($[M+Na]^+$).

Methyl 2-(4-methoxy-1H-indol-3-yl)-2-oxoacetate (5):

To a stirred solution of 4-methoxy-1H-indole (**4**) (5.0 g, 33.97 mmol) dissolved in 100 mL of anhydrous THF at 0 ^{o} C, was added oxalyl chloride (4.74 g, 37.34 mmol) dropwise, then the reaction mixture was allowed to stir for 2h at room temperature. The reaction mixture was then cooled to 0 ^{o}C, and 5 mL of MeOH was added dropwise. Then the reaction mixture was stirred overnight at room temperature.Formation of the product was confirmed by LC-MS. The reaction mixture was diluted with diethyl ether, dried over sodium sulfate, filtered and evaporated under reduced pressure to afford the desired compound **5** (3.98 g, 50.2%) as a colorless solid. The product was confirmed by ^{1}H NMR & Mass Spec.

^{1}H NMR (400 MHz, DMSO-*d6*): δ 12.37 (1H, s), 8.19 (1H, s), 7.20-7.10 (2H, m), 6.73 (1H, d, J=7.8 Hz), 3.84 (3H, s), 3.82 (3H, s). MS: *m/z* 234 ($[M+ H]^+$).

Methyl 2-(4-methoxy-1H-indol-3-yl) acetate (6):

To a stirred room temperature solution of methyl 2-(4-methoxy-1H-indol-3-yl)-2-oxoacetate (**5**) (3.98 g, 17.0 mmol) in 100 mL of dioxane/ H_2O (2:1) was added 10% palladium on activated carbon (1.6 g, 15.0 mmol) and sodium hypophosphite monohydrate (18.18 g, 171.52 mmol) simultaneously. Then the mixture was stirred for 48 h at room temperature. Completion of the reaction was confirmed by LC-MS. Then the reaction mixture was diluted with 60 mL of H_2O and filtered through a celite pad. The aqueous mixture was then extracted with ethyl acetate and dried over anhydrous Na_2SO_4. The solvent was evaporated under reduced pressure to provide a crude

residue which was purified by silica gel flash column chromatography to afford the title compound **6** (2.3 g, 61.5%) as a white solid. The product was confirmed by NMR & MS.

^{1}H NMR (400 MHz, CDCl3): δ 8.04 (1H, s), 7.06 (1H, t, J=8.0 Hz), 6.97-6.90 (2H, m), 6.46 (1H, d, J=7.9 Hz), 3.94 (2H, s), 3.86 (3H, s), 3.71 (3H, s). MS: *m/z* 220 ([M+ H]$^+$).

2-(4-Methoxy-1H-indol-3-yl) acetic acid (7):

To a stirred solution of methyl 2-(4-methoxy-1H-indol-3-yl) acetate (**6**) (2.3 g, 10.49 mmol) in 90 mL of THF/H_2O (2:1) at 0 ^{o}C was added KOH (1.76 g, 31.49 mmol) and the reaction mixture was allowed to warm to room temperature and stirred for 6h. Completion of the reaction was confirmed by LC-MS. Then volatiles were evaporated under reduced pressure and the crude product was neutralized with 1N HCl (aq). The obtained product was washed with water and dried under vacuum to afford the title compound (**7**) (1.82 g, 84.5%) that was confirmed by NMR & MS.

^{1}H NMR (400 MHz, DMSO-*d6*): δ 11.90 (1H, s), 10.81 (1H, s), 7.02 (1H, d J=2.5 Hz), 6.98-6.89 (2H, m), 6.41 (1H, dd, J=7.0 Hz, 1.4 Hz), 3.78 (3H, s), 3.73 (2H, s). MS: *m/z* 206 ([M+ H]$^+$).

N-(3-(Dimethyl amino) propyl)-2-(4-methoxy-1H-indol-3-yl) acetamide (8):

To a stirred solution of 2-(4-Methoxy-1H-indol-3-yl) acetic acid **(7)** (825 mg, 2.85 mmol) and N1,N1-dimethylpropane-1,3-diamine (**1**) (821 mg, 8.034 mmol) in 20 mL dry CH_2Cl_2 at 0 ^{o}C, (2.16 mL, 12.0 mmol) was added diisopropylethylamine (1.84 mL, 14.25 mmol) and T3P 50% solution in CH_2Cl_2 by weight (3.32g , 3.70 mmol) simultaneously by dropwise addition. Then the reaction mixture was stirred at 30 mins at 0 ^{o}C. The completion of the reaction was confirmed by LC-MS, after which the reaction mixture was quenched with cold water, and extracted with CH_2Cl_2, then dried over anhydrous Na_2SO_4, and the solvent was evaporated under reduced pressure.

The crude product was purified by flash column chromatography to afford the title compound (**8**) (890 mg, 76.5%) that was confirmed by NMR & MS.

^{1}H NMR (400 MHz, DMSO-d6): δ 10.85 (1H, s), 7.41 (1H, t, J=5.4 Hz), 7.0 (1H, d, J=2.2 Hz), 6.98-6.89 (2H, m), 6.42 (1H, dd, J=6.8 Hz, 1.7 Hz), 3.80 (3H, s), 3.58 (2H, s), 3.11-3.01 (2H, m), 2.12 (2H, t, J=7.0 Hz), 1.96 (6H, s), 1.54-1.40 (2H, m). MS: *m/z* 290 ([M+ H]$^+$).

4-Iodo-N-(3-(2-(4-methoxy-1H-indol-3-yl) acetamido) propyl)-N, N-dimethylbutan-1-aminium iodide (9):

To a stirred solution of N-(3-(Dimethyl amino) propyl)-2-(4-methoxy-1H-indol-3-yl) acetamide (**8**) (600 mg, 2.073 mmol) in 10 mL of butyronitrile at room temperature was added 1,4-diiodobutane (6.42 g, 20.71 mmol). The temperature of the reaction mixture was then raised to 50 ^{o}C and stirred for 16 h. Completion of the reaction was confirmed by LC-MS. The reaction mixture was then diluted with 50 mL diethyl ether, and the resulting precipitate was filtered and washed with diethyl ether to obtain the title compound (**9**) (890 mg, 71.5%) that was confirmed by NMR & MS.

^{1}H NMR (400 MHz, CD3OD): δ 7.12-6.97 (3H, m), 6.56 (1H, d, J=7.0 Hz), 3.90 (3H, s), 3.80 (2H, s), 3.36-3.25 (2H, m), 3.20 (2H, t, J=6.96 Hz), 3.12-2.98 (4H, m), 2.86 (6H, s), 1.93-1.80 (2H, m), 1.80-1.69 (2H,m), 1.61-1.49 (2H, m). MS: *m/z* 472 (M$^+$).

(S,Z)-N1-(6,11-bis(tert-butoxycarbonylamino)-2,2-dimethyl-4,12-dioxo-3-oxa-5,7,13-triazahexadec-5-en-16-yl)-N4-(3-(2-(4-methoxy-1H-indol-3-yl)acetamido)propyl)-N1,N1,N4,N4-tetramethylbutane-1,4-diaminium (10):

To a stirred solution of 4-Iodo-N-(3-(2-(4-methoxy-1H-indol-3-yl)acetamido)propyl)-N,N-dimethylbutan-1-aminium iodide (**9**) (800 mg, 1.33 mmol) in 15 mL of ethanol was added (S, Z)-Tert-butyl 2,17,17-trimethyl-7,15-dioxo-16-oxa-2,6,12,14-tetraazaoctadecan-8-yl-13-ylidenedicarbamate (**3**) (745 mg, 1.33 mmol) at room

temperature and reaction temperature was raised to 45 ^{o}C and stirred for 48 h. Completion of the reaction was confirmed by LC-MS. Volatiles were removed under reduced pressure to obtain crude product that was purified by reverse phase HPLC to afford the title compound (**10**) (1.2 g, 61.2%) confirmed by NMR & MS.

^{1}H NMR (400 MHz, CD3OD): δ 7.14-7.0 (3H, m), 6.56 (1H, dd, J=7.0 Hz, 1.2 Hz), 3.98 (1H, m), 3.94 (3H, s), 3.76 (2H, s), 3.40-3.23 (8H, m), 3.2-3.16 (2H, m), 3.15-3.05 (4H, m), 3.02 (6H, s), 2.91 (6H, s), 2.0-1.85 (4H, m), 1.84-1.59 (8H, m), 1.56 (4H, s), 1.53 (9H, s), 1.44 (14H, s). MS: *m/z* 452 (M^{2+}).

(S)-N1-(3-(2-amino-5-guanidino pentanamido) propyl)-N4-(3-(2-(4-methoxy-1H-indol-3-yl) acetamido) propyl)-N1, N1, N4, N4-tetramethylbutane-1,4-diaminium iodide (11):

To a stirred solution of (S,Z)-N1-(6,11-bis(tert-butoxycarbonylamino)-2,2-dimethyl-4,12-dioxo-3-oxa-5,7,13-triazahexadec-5-en-16-yl)-N4-(3-(2-(4-methoxy-1H-indol-3-yl)acetamido)propyl)-N1,N1,N4,N4-tetramethylbutane-1,4-diaminium (**10**) (60 mg, 0.052 mmol) in 2 mL dry CH_2Cl_2 at 0 ^{o}C, was added 2 mL of trifluoroacetic acid dropwise, then the reaction mixture was allowed to warm to room temperature and was stirred for 16h. Completion of the reaction was confirmed by LC-MS. Volatiles were removed under reduced pressure to obtain crude product that was purified by reverse phase HPLC to yield compound **11** (30 mg, 0.03 mmol, 67.2% %) that was confirmed by NMR & MS.

^{1}H NMR (400 MHz, CD3OD): δ 7.13-7.0 (3H, m), 6.56 91h, dd J=7.1 Hz, 1.2 Hz), 3.93 (3H, s), 3.92-3.87 (2H, m), 3.76 (2H, s), 3.50-3.07 (14H, m), 2.07-1.81 (8H, m), 1.75-1.58 (4H, m). MS: *m/z* 302 (M^{2+}).

(S)-N1-(3-(2-amino-5-guanidinopentanamido) propyl)-N4-(3-(2-(4-hydroxy-1H-indol-3-yl) acetamido) propyl)-N1, N1, N4, N4-tetramethylbutane-1,4-diaminium iodide (12):

(S,Z)-N1-(6,11-bis(tert-butoxycarbonylamino)-2,2-dimethyl-4,12-dioxo-3-oxa-5,7,13-triazahexadec-5-en-16-yl)-N4-(3-(2-(4-methoxy-1H-indol-3-yl)acetamido)propyl)-N1,N1,N4,N4-tetramethylbutane-1,4-diaminium (**10**) (30 mg, 0.026 mmol) in 2 mL anhydrous CH_2Cl_2 at -78 ^oC, was added 0.2 mL of BBr_3 dropwise and slowly, then the reaction mixture was gradually brought to room temperature over 1-2 hours and stirred for 16h. Completion of the reaction was confirmed by LC-MS. Volatiles were removed under reduced pressure to provide the crude product, **12**. Then 1 mL of MeOH was added slowly and dropwise at -78 ^oC and the mixture was slowly brought to room temperature. The crude product was purified by reverse phase HPLC to obtain the title compound (**12**) (10 mg, 0.012 mmol, 45.6%) that was confirmed by NMR & MS.

^1H NMR (400 MHz, CD3OD): δ 7.05 (1H, s), 7.0-6.9 (2H, m), 6.44 (1H, dd, J=7.0 Hz, 1.5 Hz), 3.95-3.87 (2H, m), 3.75 (2H, s), 3.5-3.05 (14H, m), 2.06-1.82 (8H, m), 1.76-1.54 (4H, m). MS: *m/z* 295 (M^{2+}).

Rodent animals

All animal experiments were treated according to the guidelines for use of animals in research approved by the Drexel University Institutional Animal Care and Use Committee (IACUC) and are in agreement with the U.S. Public Health Service Policy on Humane Care and Use of Laboratory Animals. Sprague-Dawley rats were purchased from Charles River (Malvern, PA, USA), and housed in Association for Assessment and Accreditation of Laboratory Animal Care-accredited facilities. Animal

housing and experimental procedures were also approved by the Drexel University College of Medicine Institutional Animal Care and Use Committees (IACUC).

Antibodies

Primary antibodies for immunocytochemistry were polyclonal anti-microtubule associated protein-2 (MAP-2, cat: AB5622) and monoclonal anti-glial fibrillary acidic protein (GFAP, cat: MAB360), both purchased from Millipore (Temecula, CA, USA). Secondary antibodies included Alexa Fluor® 488 conjugated AffiniPure Donkey Anti-Rabbit IgG and Cy™3-conjugated AffiniPure Donkey Anti-Mouse IgG. These antibodies, along with normal donkey serum and normal goat serum, were purchased from Jackson Immuno Research (West Grove, PA, USA).

Examination of effect of compounds in neurotransmitter uptake assays

Neurotransmitter transporter studies in cell lines

Cell Culture and DNA Transfection. COS-7 cells were maintained in DMEM containing 10% fetal bovine serum, 100 units/mL of penicillin and 100 µg/mL streptomycin in a humidified incubator with 5% CO_2 at 37 °C. MDCK cells were kept under the same conditions except that DMEM media contained 1 µg/mL blasticidin as well.

For L-glutamate, GABA and glycine uptake assays, subconfluent COS-7 cells were transiently transfected with 0.5 µg of plasmid DNA (EAAT1, EAAT2, EAAT3, GAT-1, GAT-3, GlyT1 and GlyT2) per well using TransIT-LT1 transfection reagent (Mirus Bio LLC, Madison, WI, USA), and plated at a density of 50,000 cells/well and uptake experiments were performed two days after plating. Transfection with empty vector pCMV-5 was used to control for the level of endogenous uptake of radiolabelled

substrate in each experimental condition. Additionally, background for GABA uptake assays was examined in using nipecotic acid, and for glycine uptake assays using sarcosine and *N*-arachidonylglycine.

For monoamine transporters assays, stable MDCK cells expressing hNET (human noradrenaline transporter), hDAT (dopamine transporter) and hSERT (serotonin transporter) were used. Naïve MDCK cells were used for obtaining the background. Cells were plated in 96-well plates at density of 50,000 cells/well and uptake experiments were performed one day after plating.

Dose-response assays. Neurotransmitter uptake assays were performed as previously reported[81, 136]. Briefly, cells were washed with room temperature phosphate buffer PBS-CM (2.7 mM KCl; 1.2 mM KH_2PO_4, 138 mM NaCl; 8.1 mM Na_2HPO_4, added 0.1 mM $CaCl_2$ and 1 mM $MgCl_2$, pH 7.4) and incubated for 10 min at 37 ^oC with several concentrations of compounds: Pwx2 fraction or commercial FrPbAII (1 - 500 µM), arginine, betaine, homarine, L-carnitine hydrochloride, spermidine trihydrochloride and spermine (0.01 nM- 100 µM), natural Pwx10 fraction or synthetic (compounds 10 and 12 in figures 7-8), at 0.1 –1 mM final concentrations. Uptake reactions were initiated by the addition of appropriate radiolabelled substrate (^{3}H-L-glutamate, GABA or glycine) at final concentration of 50 nM. After 10 min, uptake was terminated by removal of solution, followed by two washes with PBS-CM and lysis with 1% SDS/0.1 M NaOH for 20 min. The lysate was transferred to scintillation vials containing 3 mL of scintillation fluid (ScintiVerse, Fisher Scientific, Pittsburgh, PA, USA) and radioactivity was quantified in a scintillation counter LS 6500 (Beckman Coulter, Brea, CA).

For monoamine transport assays in MDCK cells plated in 96-well plates, we used ^{3}H- serotonin or dopamine at 50 nM final concentration. Uptakes were performed

similarly as above, expect that an Elx50® Biotek plate washer (Winooski, VT, USA) was used for washes. After termination of uptakes, scintillation fluid was added to each well, and the plates were counted in a Wallac M50 microbeta scintillation analyser (Perkin Elmer, Boston, MA, USA).

Kinetic assays. For kinetic assays, COS-7 cells were transfected with wild type (WT) EAAT1, EAAT2 or empty vector, as described above. Two days later, plates were pre-incubated with Pwx10 fraction or compounds 11 and 12 (figures 7-8) for 10 min at the indicated concentrations. Uptake reactions were initiated by the addition of unlabelled L-glutamate and ^{3}H-L-glutamate (1–1000 μM, final concentration, 99% unlabelled and 1% labelled). After 10 minutes, uptake was terminated and radioactivity counted as above.

Glutamate transporter studies in astrocytes

Astrocyte preparation. Glia was prepared and cultured according a previous study[108], with modifications. Briefly, cerebral cortices from 2-4 day old Sprague-Dawley rat pups were dissected under sterile conditions and placed in 60 mm dishes containing dissection medium (in mM: Glucose 16, Sucrose 22, NaCl 135, KCl 5, Na_2HPO_4 1, KH_2PO_4 0.22, HEPES 10, pH 7.4, Osmolarity 310+10 mOsm). Tissue was minced with curved scissors, digested in 0.25% trypsin for 15 min. Trypsin action was ended by transferring tissue pieces to another vial with dissection medium. Tissue was then repeatedly passed through a serological plastic pipette until dissociated by trituration in presence of 60 μg/mL DNAse. Cells were pelleted by centrifugation for 15 minutes at 280 x g, and resuspended in glia plating medium (90% DMEM, 10% FBS and 50 μg/mL gentamicin) and transferred to culture flasks to a 37 °C incubator

(5-10% CO_2). After growth for 10 days in vitro (DIV), cells were detach with 0.05% trypsin, centrifuged and plated at the density of 10,000 cells/well in poly-lysine coated 96-well plates. Plates are grown for 14 DIV before uptake assays.

Uptake assays. Assays were performed as described[109]. Briefly, using an Elx50® Biotek plate washer (Winooski, VT, USA), cells are washed in PBS-CM buffer. For dose response assays, vehicle and several concentrations of compounds 11 and 12 (shown in figures 7-8, at 0.01 nM- 1 μM) were added and incubated for 10 min at 37°C. Uptake assays are initiated by addition of 50 nM L- [^{3}H]-glutamate, and incubation is carried on for 10 min at room temperature. Non-specific uptake was obtained in presence of 10 μM DL-TBOA.

For kinetic assays, cells are washed in PBS-CM buffer and pre-incubated in the presence of either vehicle or several concentrations of the compounds, uptake reactions are initiated by the addition of unlabeled L-glutamate and ^{3}H-L-glutamate (1–1000 μM, final concentration, 99% unlabeled and 1% labeled). Incubation was carried on for 10 min at room temperature. Non-specific uptake was also obtained in presence of DL-TBOA.

Reactions were finished by washing the plates twice with PBS-CM and the addition of 100 μL of scintillation fluid to each well. Radioactivity was counted in a Microplate Scintillation and Luminescence Counter (Wallac, Shelton, CT, USA).

Examination of the effect of compounds in primary mixed neuron-glia cultures

In this work, we have examined the effects of both Pwx10 fraction and synthetic (compounds **11** and **12** in figures 7-8) in two models of excitotoxicity in primary neuron-glia cultures.

Mixed neuron-glia cultures

Cortical cells were obtained from late embryonic stage (E17) Holtzman rats. These cells were plated at a density of 35,000 cells/coverslip in 12-well plates for immunocytochemistry assays as previously described[82].

We did not add AraC to mixed neuron-glia cultures. Culture conditions were optimized to contain enough glia to observe suitable expression of EAAT1 and EAAT2 and treatment effects of compounds, while maintaining a population of neurons that is large enough to accurately measure neuronal survival, as previously described[82]. This was achieved by plating cells in Neurobasal media (NB) with 2% B27 supplement and 10% Horse Serum. The media was changed 2 h after plating to NB media containing 2% B27, 2% Horse serum, 1% glutamine, 25 μM L-glutamate and 50 μg/mL gentamicin. 4 days later, media was changed to NB media with 2% B27, 1% glutamine and 50 μg/mL gentamicin. Finally, cells received fresh NB media (with 2% B27, 1% glutamine and 50μg/mL gentamicin) at 8 DIV, and cultures were exposed to excitotoxic insults and compound treatment at 14 DIV. At 14 DIV, cultures are well-differentiated, markers of neuronal maturity, such as NeuN; NF-L; NF-M; GAD; TH; PSD-95 and synaptophysin, are well expressed[137]; protein content and mitochondrial respiration is stabilized[138-139]; and L-glutamate receptors are well expressed[118, 140-142], as well as L-glutamate transporters[82].

These growth conditions produced approximately 15% glia in each culture[82], and only cultures with consistent percentages of astrocytic populations across individual experiments and coverslips were included in the study. Any culture with a proportion of glia that was significantly different from a range of 7-18% (measured by One-Way

ANOVA followed by Newman-Keuls *post hoc* test for multiple comparisons performed on the percentage of GFAP+ in each coverslip) was excluded from the analysis.

Excitotoxic insult models

L-glutamate mediated excitotoxic insults and compound administration

At 14 DIV, cultures were examined before each experiment for cell viability under a TCM-BR inverted bright field microscope. Cultures that appeared unhealthy were discarded from further experiments. L-Glutamate and compound solutions were made in fresh growth media. L-glutamate (100 μM) was directly added to the mixed cultures for 24h. Pwx10 fraction and compound **12** (figure 8), were co-applied at 1, 10 or 100 nM concentrations, and allowed to incubate for 24h. Additionally, as positive control for neuroprotection, some cultures were treated with 100 μM APV, an NMDA receptor blocker, which was added at the same time as the 100 μM L-glutamate insult. Also, to evaluate the effect of blockage of L-glutamate transport, some cultures were treated with the non-selective L-glutamate transporter blocker DL-TBOA (100 μM) or the EAAT2 specific inhibitor WAY 213613 (1 μM). These compounds were also added at the same time as the L-glutamate insult.

Additionally, to test for any possible toxicity of the experimental compounds, cultures were treated with Pwx10 fraction or with compound **12** (figure 8) at 100 nM for 24 hours, without any insults.

Oxygen-Glucose Deprivation (OGD) insults and compound administration

We extended our studies to evaluate the effects of Pwx10 fraction and compound **12** (figure 8) after OGD insults, an *in vitro* stroke model[19, 143]. Glucose-free

DMEM (OGD media) and regular growth media were warmed in 37°C water bath. A hypoxic chamber (Billups-Rothenberg, San Diego, CA, USA) was sterilized in UV light for 20 min prior to the experiment, and pre-warmed OGD media was de-gassed for 5 min by bubbling with a gas mixture composed of 10% H_2/85% N_2/5 %CO_2 or 95% N_2/5% CO_2. The media on the cultures was replaced with 1 mL/well/ coverslip of de-gassed OGD media. Plates were placed in the hypoxic chamber and were de-gassed for 5 min. The chamber was then sealed and put in the 37 °C incubator for 15 min, resulting in a 20 min insult. The choice for this insult time was based on previous experiments that showed that these conditions resulted in ~50% of neuronal death, i.e., they were appropriate to study the effect of compounds on neuronal survival (Figure 10). Following the OGD insult, cultures were either incubated with fresh growth media (vehicle control), several concentrations of Pwx10 fraction or compound **12**, 100 μM APV, 100 μM TBOA, or 1 μM WAY 213613 as post-treatments.

Immunocytochemistry assays for evaluation of neuronal survival

To evaluate neuronal health status (as a function of MAP-2) and the effect of treatment with compounds, cultures on 15 mm glass coverslips were fixed and fluorescently labelled as described[144-146]. As a control for initial levels of neuronal survival, cultures not subjected to treatments (time zero) were also examined. Briefly, cultures on coverslips were fixed with 2% paraformaldehyde, permeabilized with 0.1% Triton X-100, blocked with 5% Normal Donkey serum, washed and incubated overnight with primary antibodies in 5% blocking solution: anti-MAP-2 (1:1,000) and anti-GFAP (1:400). Then the following secondary antibodies were added: Alexa Fluor® 488 conjugated AffiniPure Donkey Anti-Rabbit IgG for MAP-2 detection and Cy™3-conjugated AffiniPure Donkey Anti-Mouse IgG for GFAP, both at 1:500,

prepared in blocking solution (5% normal donkey serum in PBS). After 30 min incubation in the dark, coverslips were washed and mounted on a slide with ProLong® Diamond Antifade Mountant with DAPI Thermo Fisher Scientific (Waltham, MA, USA) for nuclear staining. Coverslips were then sealed with clear nail polish.

Image acquisition and neuronal survival counting

Cells were imaged with a fluorescent microscope to examine morphology and a confocal microscope to quantify cell survival. We used the following settings for the confocal microscope: quality: 1280x1024, 2.4x analog gain, and dynamic contrast. The exposure was set at 8 seconds and images were taken using the 30x zoom setting. For all experiments, 5-10 random fields/coverslip and 3-4 coverslips were evaluated per treatment condition. Images were taken in all 3 filters to visualize DAPI, Alexa-488 (for MAP-2), and Cy3 (for GFAP). For assessment of cell population, cells in the cultures were classified into neurons (MAP-2 positive cells) and glia (GFAP positive cells). The abundance of each cell type was calculated and expressed as percent of total, DAPI positive cells on a coverslip.

Neuronal survival was evaluated by in a blind manner. Survival was determined by evaluating individual neurons for features that are indicative of neurodegeneration and apoptosis, such as pyknotic nuclei, membrane blebbing, and neuritis[146-147]. Nuclei that stained with DAPI but lacked significant MAP-2 staining were also classified as dead neurons. The percentage of neuronal survival was calculated by dividing the number of MAP-2 positive neurons with no morphological signs of toxicity, by the total number of MAP-2 positive neurons on each coverslip.

For each experimental condition, 5 random fields from 3-4 coverslips were analysed, totalling at least 100-150 neurons. Mean survival in each treatment condition was normalized to mean survival in the control group for each experiment. The normalization was performed considering the control group of each individual experiment as 100% of survival and obtaining the relative percentage of neuronal survival of each condition/treatment. Additionally, neuronal survival was evaluated before all insults (time zero) in at least 4 control coverslips, before beginning each experiment. Only sets of experiments with reasonable survival rates at time zero (>75%) were included in the final analysis of neuronal survival.

Images were processed using ImageJ® from the National Institute of Health (Bethesda, MD, USA).

Data analysis

All data were analyzed using GraphPad Prism version 5.03 for Windows (GraphPad Software, La Jolla, CA, USA).

Data generated from dose-response assays on the effects of the compounds on L-glutamate, GABA, glycine and monoamine transport were fitted to a dose-response curve by non-linear regression analysis using GraphPad Prism version 5.03 for Windows. Non-specific transport (background) for L-glutamate uptake in COS-7 cells was transfected with an empty vector (pCMV). For GABA uptakes, we obtained the background in the presence of specific GABA transport inhibitor nipecotic acid (1 mM, final concentration), and for glycine uptake, in presence of sarcosine (GAT-1 transport inhibitor, 100 μM, final concentration) or N-Arachidonylglycine (specific GAT-3 inhibitor, 100 μM, final concentration). For L-glutamate uptakes in glia plated in 96 well plates, wells received DL-TBOA (100 μM final concentration) to obtain the

background. For monoamine transporter assays in stable transfected MDCK cells, naïve MDCK cells were used to obtain the background. Background values were subtracted from the total. EC_{50} and IC_{50} values (as the concentration of compound resulting in 50% of the maximum observed stimulation or inhibition, respectively), and efficacies are given as means ± SEM of three or four independent assays performed in triplicate, and normalized to percentage of control (vehicle).

Michaelis-Menten kinetics was assumed for calculation of K_m and $V_{max.}$ Statistical significance was assessed using One-way analysis of variance (ANOVA) followed by Dunnett's or Bonferroni multiple comparisons *post hoc* tests with vehicle (for analysis of the effect of compounds) as control (* p <0.05). Background values were obtained either by CMV-expressing COS-7 cells or in presence of DL-TBOA (for glia uptakes), those values were subtracted for calculation of specific uptake values.

For neuroprotection studies, the neuronal survival was expressed as % of neuronal death comparing control, insult and treatments. Statistical significance was assessed using One-way analysis of variance (ANOVA) followed by Dunnett's multiple-comparisons *post hoc* test with vehicle as control (* p < 0.05), or Newman-Keuls *post hoc* test for multiple comparisons (# p < 0.05).

Supporting information

MS/MS spectra of all compounds identified from the *P. bistriata* venom, NMR and MS spectra for all compounds leading to synthesis of 4-OH-IndAc3(Me_2)4(Me_2)3Arg^{2+}, activity of constituents of the fraction Pwx2 on GABA and glycine transporters; lack of bioactivity of Pwx10 fraction and compounds **11** and **12** on GABA, glycine and monoamine transporters, and L-glutamate uptake in mixed neuron-glia cultures in presence of specific inhibitors.

Abbreviations used

ALS, Amyotrophic Lateral Sclerosis; AMPA, α-amino-3-hydroxy-5-methyl-4-isoxazolepropionic acid; APV, (2R)-amino-5-phosphonovaleric acid; AraC, Cytosine-β−D-arabinofuranoside; CNS, Central Nervous System; DAPI, 4',6-Diamidino-2-Phenylindole; DCM, dichloromethane; DIV, Days in vitro; DL-TBOA, DL- threo-β-Benzyloxyaspartic acid; DMF, dimethylformamide; D-PBS, Dulbecco's phosphate-buffered saline; PBS-CM, D-PBS with 0.1 mM $CaCl_2$ and 1 mM $MgCl_2$ added; EAAT1-5, Excitatory amino acid transporters 1-5, respectively; GAT-1, GABA transporter subtype 1, GAT-3, GABA transporter subtype 3; GlyT1, glycine transporter subtype 1; GlyT2, glycine transporter subtype 2; GLAST; glutamate aspartate transporter, rodent homologue of EAAT1, GLT-1, glutamate transporter 1, rodent homologue of EAAT2; EAAC1, excitatory amino acid carrier 1, rodent homologue of EAAT3; GFAP, Glial Fibrillary Acidic Protein; ESI-HR-MS/MS, electionspray ionization high-resolution tandem mass spectrometry; MAP-2, mGluR, metabotropic glutamate receptor; Microtubule-Associated Protein 2; NAM, negative allosteric modulation; NB media, Neurobasal media; NMDA, N-methyl-D-aspartate; NaOH, sodium hydroxide; OGD, Oxygen-glucose deprivation; PAM, positive allosteric modulation; Pwx10, Parawixin10; SDS, sodium dodecyl sulphate; SKF 89976A hydrochloride, 1-(4,4-Diphenyl-3-butenyl)-3-piperidinecarboxylic acid hydrochloride; UCPH 101, 2-Amino-5,6,7,8-tetrahydro-4-(4-methoxyphenyl)-7-(naphthalen-1-yl)-5-oxo-4H-chromene-3-carbonitrile; UHPLC, ultra-high performance liquid chromatography; WAY 213613, N-[4-(2-Bromo-4,5-difluorophenoxy)phenyl]-L-asparagine; WT, wild type.

Author information

Author contributions

Project design and search for funding: J.L.L., W.F.S, J.M.S., L.B., S.B. and A.C.K.F. Venom collection: J.L.L, W.F.S. Compound isolation: J.L.L, W.F.S, Y.M.F, S.B., L.B. Structure elucidation: Y.M.F, S.B., L.B. Chemical synthesis: P.A.N.R, J.M.S. Bioassays: J.L.G., A.K, W.F.S. and A.C.K.F. Manuscript writing: Y.M.F., J.M.S., L.B., W.F.S. and A.C.K.F.

Conflict of interests

None.

Funding sources

This work was supported by São Paulo State Research Foundation (FAPESP, Brazil) to W.F.S. (grants number 2014/21419-2 and 2005/60254-0). Brazilian National Council for Scientific and Technological Development (CNPq) and Coordination for the Improvement of Higher Education Personnel (CAPES) sponsored J.L.L.

Acknowledgments

The authors wish to thank Ole. V. Mortensen for helpful discussions (Department of Pharmacology and Physiology, Drexel University) and Dominique Kamber (Department of Chemistry, University of Zurich) for the synthesis of homarine reference material.

Figure legends

Figure 1: Base peak chromatogram (BPC) of the P. bistriata venom with indication of the peaks related to previously isolated neuroprotective fractions Pwx2 and Pwx10.

Figure 2: The MS/MS spectrum of the precursor ion *m/z* 175.12 $[M+H]^+$ found in the crude venom of *P. bistriata* (top) compared to the MS/MS spectra recorded from the commercial reference material FrPbAII (left) and arginine (right) proving that the spider venom contains in fact arginine but not FrPbAII.

Figure 3: Uptake assays in COS-7 cells transfected with GABA transporters GAT-1 and GAT-3 and glycine transporters GlyT1 and GlyT2 reveal that natural fraction Pwx2 inhibits GABA uptake specifically through GAT-1. A. Dose-response curves of Pwx2 fraction, B. Dose response curves of commercial FrPbAII, C. Dose-response curves of arginine, D. Effects of nipecotic acid (1 mM) on both GAT-1 and GAT-3 transporters and specific GlyT1 inhibitor sarcosine and GlyT2 inhibitor N-Arachidonyl-glycine (100 mM) on glycine transporters. COS-7 cells transiently transfected with appropriate cDNA or empty vector were pre-incubated for 10 min with varied concentrations of compounds and reactions with 50 nM of ^{3}H-GABA or ^{3}H-glycine were carried out for 10 min. Results are normalized to percentage of control (vehicle) and expressed as mean ± SEM of three independent experiments.

Figure 4: Full scan (FS)-MS of the peak in the UHPLC-MS chromatogram of the *P. bistriata* crude venom (6.78 – 6.92 min), which corresponds to the doubly charged ion *m/z* 294.7 (main signal detected for the Pwx10 fraction).

Figure 5: The acylpolyamine 4-OH-IndAc3(Me_2)4(Me_2)3Arg^{2+}; identified from the MS/MS spectrum of the precursor ion *m/z* 816.4 with fragment ion annotation.

Figure 6: Schematic overview for the free polyamines and acylpolyamines found in the venom of *P. bistriata*. For nomenclature and structures please see supplementary material.

Scheme 1: Synthesis scheme leading to 4-OH-IndAc3(Me_2)4(Me_2)3Arg^{2+}; (shown as compound **12**).

Scheme 2: Synthesis scheme of 4-OH-IndAc3(Me_2)4(Me_2)3Arg^{2+}; (compound **12**).

Figure 7: Fraction Pwx10 stimulates both EAAT1 and EAAT2-mediated transport.

A. Dose response of Pwx10 fraction on L-glutamate transport mediated by EAAT1, EAAT2 or EAAT3 shows that the compound does not modulate EAAT3-mediated transport but increases EAAT1 and EAAT2; EC_{50s} and efficacies are indicated. Cells were incubated with varied concentrations of compound for 10 min at 37 ^{o}C and 10 min with 50 nM ^{3}H-L-glutamate. Results are normalized to percentage of control

(vehicle) and expressed as mean ± SD of three independent experiments, B. Pwx10 fraction augments L-glutamate uptake in a native environment of culture astrocytes. Cells were incubated with varied concentrations of compound for 10 min at 37 ^{o}C and 10 min with 50 nM ^{3}H-L-glutamate. Results are normalized to percentage of control (vehicle) and expressed as Mean ± SD of all the experiments, C. Effects of Pwx10 fraction (10, 100 and 500 nM) on the kinetics of EAAT1, and D. Effects of Pwx10 fraction (10, 100 and 500 nM) on the kinetics of EAAT2. V_{max} and K_M were calculated, and the values are presented in the table; K_M was not statistically different between the varying concentrations of compounds analysed in this study, *** $p < 0.001$, V_{max} comparing compound (100 and 500 nM) to vehicle. Assays were performed in COS-7 cells transiently transfected with appropriate cDNA or empty vector, E. Kinetic analysis of L-glutamate uptake in cultured glia cells pre-incubated with vehicle, 100 nM and 500 nM of Pwx10 fraction. V_{max} and K_M were calculated, and values are presented in the table; K_M was not statistically different between treatments, ***$p < 0.001$, V_{max} comparing compound to vehicle.

Figure 8: Compounds **11** and **12** have similar activities to fraction Pwx10, modulating EAAT1 and EAAT2 transporter activities.

Dose responses of **12** (A) and **11** (B) on L-glutamate transport mediated by EAAT1, EAAT2 or EAAT3 shows that the compounds do not modulate EAAT3-mediated transport but increase EAAT1 and EAAT2; EC_{50s} and efficacies are indicated. Cells were incubated with varied concentrations of compound for 10 min at 37 ^{o}C and 10 min with 50 nM ^{3}H-L-glutamate. Results are normalized to percentage of control (vehicle) and expressed as mean ± SD of three independent experiments, C. **12** and

11 augment L-glutamate uptake in a native environment of culture astrocytes. Cells were incubated with varied concentrations of compounds for 10 min at 37 ^{o}C and 10 min with 50 nM ^{3}H-L-glutamate. Results are normalized to percentage of control (vehicle) and expressed as Mean ± SD of all the experiments, D. Effects of **12** and **11** (100 and 500 nM) on the kinetics of EAAT1, and E. Effects of **12** and **11** (100 and 500 nM) on the kinetics of EAAT2. V_{max} and K_M were calculated, and the values are presented in the table; K_M was not statistically different between the varying concentrations of compounds analysed in this study, *** $p < 0.001$, V_{max} comparing compound (100 and 500 nM) to vehicle. Assays were performed in COS-7 cells transiently transfected with appropriate cDNA or empty vector, F. Kinetic analysis of L-glutamate uptake in cultured glia cells pre-incubated with vehicle, 100 nM and 500 nM of **12** and **11**. V_{max} and K_M were calculated, and values are presented in the table; K_M was not statistically different between treatments, ***$p < 0.001$, V_{max} comparing compound to vehicle.

Figure 9: Neuroprotective properties of Pwx10 fraction and 4-OH-IndAc3(Me_2)4(Me_2)3Arg^{2+} (**12**) in mixed neuron-glia cultures after prolonged exposure to L-glutamate.

A. Representative Images of 14 DIV mixed neuron-glia cultures in control conditions, after treatments with 100 µM Pwx10 fraction or 100 µM L-glutamate, and after treatment with 100 µM L-glutamate in presence of 100 nM Pwx10 fraction, for 24 h. Cells were fixed and immunostained for the neuronal marker MAP-2 (green) and the glial marker GFAP (red), and counterstaining with the nuclear marker DAPI (blue). Vehicle and Pwx10 fraction treated cultures in the absence of L-glutamate do not

display obvious degeneration of cell death. Cell death was evident in L-glutamate treated cultures, as assessed by the increased number of DAPI positive, MAP-2 and GFAP negative cells. Co-treatment with 100 nM Pwx10 fraction reversed a portion of the L-glutamate toxicity by increasing MAP-2 and GFAP expression and reducing the number of DAPI-only cells. All images are shown at 40x magnification. Scale bar: 100 µm.

B: Quantification of neuronal survival (normalized to control, vehicle-treated cultures). L-glutamate significantly reduced neuronal survival, which was mitigated by co-treatment with Pwx10 fraction and **12 (**100 nM) and the NMDA antagonist APV. Co-treatment with Pwx10 fraction (100 nM) and the L-glutamate transporter inhibitor TBOA or the selective EAAT2 inhibitor WAY 23 213613 did not rescue neuronal damage in L-glutamate exposed cultures, suggesting that 4-OH-IndAc3(Me_2)4(Me_2)3Arg^{2+} -mediated neuroprotection requires active L-glutamate transporters. 3-4 coverslips were assessed per treatment condition, and 100-150 cells were manually counted per treatment. Neuronal survival data is representative of 3 independent experiments (n=9) and control levels were not statistically different for normalization purposes. ***p <0.001, **p <0.01, *p <0.05, vs. control (no insult), ###p <0.001, vs. insult, &p <0.05 Pwx10 (100 nM) + TBOA (100 mM) vs. Pwx10 fraction (100 nM) + WAY 213613 (1 mM).

Figure 10: Neuroprotective properties of Pwx10 fraction and 4-OH-IndAc3(Me_2)4(Me_2)3Arg^{2+} (**12)** in mixed neuron-glia cultures after transient oxygen and glucose deprivation.

A. Representative Images of 14 DIV mixed neuron-glia cultures in control conditions, after 20 min OGD insult and after OGD insult followed by treatment with 100 μM Pwx10 fraction, for 24 h. Cells were fixed and immunostained for the neuronal marker MAP-2 (green) and the glial marker GFAP (red), and counterstaining with the nuclear marker DAPI (blue). Vehicle cultures in the absence of OGD insult do not display obvious degeneration of cell death. Cell death was evident after OGD insult, as assessed by the increased number of DAPI positive, MAP-2 and GFAP negative cells. Post-treatment with 100 nM Pwx10 fraction or **12** reversed a portion of the L-glutamate toxicity by increasing MAP-2 and GFAP expression and reducing the number of DAPI-only cells. All images are shown at 40x magnification. Scale bar: 100 μm.

B. Quantification of neuronal survival (normalized to control, vehicle-treated cultures). OGD insult for 20 min significantly reduced neuronal survival, which was mitigated by co-treatment with 10 and 100 nM Pwx10 fraction and 100 nM **12** and the NMDA antagonist APV. The 10 and 100 nM concentration of Pwx10 fraction showed a more significant neuroprotective effect than the 1 nM concentration. Post-treatment with 100 nM Pwx10 fraction and the L-glutamate transporter inhibitor TBOA and the selective EAAT2 inhibitor WAY 23213613 did not rescue neuronal damage in L-glutamate exposed cultures, suggesting that 4-OH-IndAc3(Me_2)4(Me_2)3Arg^{2+} (**12**) –mediated neuroprotection requires active L-glutamate transporters. 3-4 coverslips were assessed per treatment condition, and 100-150 cells were manually counted per treatment. Neuronal survival data is representative of 3 independent experiments (n=9) and control levels were not statistically different for normalization purposes. ****p* <0.001, **p* <0.05, vs. control (no insult), ###*p* <0.001, vs. insult.

References

1. Fontana, A. C.; Cairrao, M. A.; Colusso, A. J.; Santos, W. F.; Coutinho-Netto, J., Paralizing activity of the Parawixia bistriata crude venom in termites: a new bioassay. *Toxicon* **2000,** *38* (1), 133-8.
2. Usherwood, P. N.; Machili, P., Chemical transmission at the insect excitatory neuromuscular synapse. *Nature* **1966,** *210* (5036), 634-6.
3. Osborne, R. H., Insect neurotransmission: neurotransmitters and their receptors. *Pharmacol Ther* **1996,** *69* (2), 117-42.
4. Fontana, A. C.; Guizzo, R.; de Oliveira Beleboni, R.; Meirelles, E. S. A. R.; Coimbra, N. C.; Amara, S. G.; dos Santos, W. F.; Coutinho-Netto, J., Purification of a neuroprotective component of Parawixia bistriata spider venom that enhances glutamate uptake. *Br J Pharmacol* **2003,** *139* (7), 1297-309.
5. Chi, H.; Chang, H.-Y.; Sang, T.-K., Neuronal Cell Death Mechanisms in Major Neurodegenerative Diseases. *International journal of molecular sciences* **2018,** *19* (10), 3082-100.
6. Wang, Y.; Qin, Z. H., Molecular and cellular mechanisms of excitotoxic neuronal death. *Apoptosis* **2010,** *15* (11), 1382-402.
7. Palmer, A. M.; Marion, D. W.; Botscheller, M. L.; Swedlow, P. E.; Styren, S. D.; DeKosky, S. T., Traumatic brain injury-induced excitotoxicity assessed in a controlled cortical impact model. *J Neurochem* **1993,** *61* (6), 2015-24.
8. Brown, J. I.; Baker, A. J.; Konasiewicz, S. J.; Moulton, R. J., Clinical significance of CSF glutamate concentrations following severe traumatic brain injury in humans. *J Neurotrauma* **1998,** *15* (4), 253-63.
9. Vespa, P.; Prins, M.; Ronne-Engstrom, E.; Caron, M.; Shalmon, E.; Hovda, D. A.; Martin, N. A.; Becker, D. P., Increase in extracellular glutamate caused by reduced cerebral perfusion pressure and seizures after human traumatic brain injury: a microdialysis study. *J Neurosurg* **1998,** *89* (6), 971-82.
10. Baker, A. J.; Moulton, R. J.; MacMillan, V. H.; Shedden, P. M., Excitatory amino acids in cerebrospinal fluid following traumatic brain injury in humans. *J Neurosurg* **1993,** *79* (3), 369-72.
11. Nilsson, P.; Hillered, L.; Ponten, U.; Ungerstedt, U., Changes in cortical extracellular levels of energy-related metabolites and amino acids following concussive brain injury in rats. *J Cereb Blood Flow Metab* **1990,** *10* (5), 631-7.
12. Yamamoto, T.; Rossi, S.; Stiefel, M.; Doppenberg, E.; Zauner, A.; Bullock, R.; Marmarou, A., CSF and ECF glutamate concentrations in head injured patients. *Acta Neurochir Suppl* **1999,** *75*, 17-9.
13. Matute, C.; Domercq, M.; Sanchez-Gomez, M. V., Glutamate-mediated glial injury: mechanisms and clinical importance. *Glia* **2006,** *53* (2), 212-24.
14. Sullivan, P. G.; Keller, J. N.; Mattson, M. P.; Scheff, S. W., Traumatic brain injury alters synaptic homeostasis: implications for impaired mitochondrial and transport function. *J Neurotrauma* **1998,** *15* (10), 789-98.
15. Seal, R. P.; Amara, S. G., Excitatory amino acid transporters: a family in flux. *Annu Rev Pharmacol Toxicol* **1999,** *39*, 431-56.
16. Jabs, R.; Seifert, G.; Steinhauser, C., Astrocytic function and its alteration in the epileptic brain. *Epilepsia* **2008,** *49 Suppl 2*, 3-12.
17. Yatomi, Y.; Tanaka, R.; Shimura, H.; Miyamoto, N.; Yamashiro, K.; Takanashi, M.; Urabe, T.; Hattori, N., Chronic brain ischemia induces the expression of glial glutamate transporter EAAT2 in subcortical white matter. *Neuroscience* **2013,** *244*, 113-21.

18. Hazell, A. S., Excitotoxic mechanisms in stroke: an update of concepts and treatment strategies. *Neurochem Int* **2007,** *50* (7-8), 941-53.
19. Lipski, J.; Wan, C. K.; Bai, J. Z.; Pi, R.; Li, D.; Donnelly, D., Neuroprotective potential of ceftriaxone in in vitro models of stroke. *Neuroscience* **2007,** *146* (2), 617-29.
20. Chu, K.; Lee, S. T.; Sinn, D. I.; Ko, S. Y.; Kim, E. H.; Kim, J. M.; Kim, S. J.; Park, D. K.; Jung, K. H.; Song, E. C.; Lee, S. K.; Kim, M.; Roh, J. K., Pharmacological Induction of Ischemic Tolerance by Glutamate Transporter-1 (EAAT2) Upregulation. *Stroke* **2007,** *38* (1), 177-82.
21. Sheldon, A. L.; Robinson, M. B., The role of glutamate transporters in neurodegenerative diseases and potential opportunities for intervention. *Neurochem Int* **2007,** *51* (6-7), 333-55.
22. Coutinho-Netto, J.; Abdul-Ghani, A. S.; Collins, J. F.; Bradford, H. F., Is glutamate a trigger factor in epileptic hyperactivity? *Epilepsia* **1981,** *22* (3), 289-96.
23. Vishnoi, S.; Raisuddin, S.; Parvez, S., Glutamate Excitotoxicity and Oxidative Stress in Epilepsy: Modulatory Role of Melatonin. *J Environ Pathol Toxicol Oncol* **2016,** *35* (4), 365-374.
24. Louzada-Junior, P.; Dias, J. J.; Santos, W. F.; Lachat, J. J.; Bradford, H. F.; Coutinho-Netto, J., Glutamate release in experimental ischaemia of the retina: an approach using microdialysis. *J Neurochem* **1992,** *59* (1), 358-63.
25. Sisk, D. R.; Kuwabara, T., Histologic changes in the inner retina of albino rats following intravitreal injection of monosodium L-glutamate. *Graefes Arch Clin Exp Ophthalmol* **1985,** *223* (5), 250-8.
26. Faden, A. I.; Demediuk, P.; Panter, S. S.; Vink, R., The role of excitatory amino acids and NMDA receptors in traumatic brain injury. *Science* **1989,** *244* (4906), 798-800.
27. Tanaka, K.; Watase, K.; Manabe, T.; Yamada, K.; Watanabe, M.; Takahashi, K.; Iwama, H.; Nishikawa, T.; Ichihara, N.; Kikuchi, T.; Okuyama, S.; Kawashima, N.; Hori, S.; Takimoto, M.; Wada, K., Epilepsy and exacerbation of brain injury in mice lacking the glutamate transporter GLT-1. *Science* **1997,** *276* (5319), 1699-702.
28. Rothstein, J. D.; Van Kammen, M.; Levey, A. I.; Martin, L. J.; Kuncl, R. W., Selective loss of glial glutamate transporter GLT-1 in amyotrophic lateral sclerosis. *Ann Neurol* **1995,** *38* (1), 73-84.
29. Dunlop, J.; Beal McIlvain, H.; She, Y.; Howland, D. S., Impaired spinal cord glutamate transport capacity and reduced sensitivity to riluzole in a transgenic superoxide dismutase mutant rat model of amyotrophic lateral sclerosis. *J Neurosci* **2003,** *23* (5), 1688-96.
30. Rothstein, J. D.; Martin, L. J.; Kuncl, R. W., Decreased glutamate transport by the brain and spinal cord in amyotrophic lateral sclerosis. *N Engl J Med* **1992,** *326* (22), 1464-8.
31. Mehta, A.; Prabhakar, M.; Kumar, P.; Deshmukh, R.; Sharma, P. L., Excitotoxicity: bridge to various triggers in neurodegenerative disorders. *Eur J Pharmacol* **2013,** *698* (1-3), 6-18.
32. Hardy, J.; Cowburn, R.; Barton, A.; Reynolds, G.; Lofdahl, E.; O'Carroll, A. M.; Wester, P.; Winblad, B., Region-specific loss of glutamate innervation in Alzheimer's disease. *Neurosci Lett* **1987,** *73* (1), 77-80.
33. Massieu, L.; Garcia, O., The role of excitotoxicity and metabolic failure in the pathogenesis of neurological disorders. *Neurobiology (Bp)* **1998,** *6* (1), 99-108.

34. Estrada-Sanchez, A. M.; Rebec, G. V., Corticostriatal dysfunction and glutamate transporter 1 (GLT1) in Huntington's disease: interactions between neurons and astrocytes. *Basal Ganglia* **2012,** *2* (2), 57-66.
35. Maeda, S.; Kawamoto, A.; Yatani, Y.; Shirakawa, H.; Nakagawa, T.; Kaneko, S., Gene transfer of GLT-1, a glial glutamate transporter, into the spinal cord by recombinant adenovirus attenuates inflammatory and neuropathic pain in rats. *Mol Pain* **2008,** *4*, 65-78.
36. Sabri, F.; Titanji, K.; De Milito, A.; Chiodi, F., Astrocyte activation and apoptosis: their roles in the neuropathology of HIV infection. *Brain Pathol* **2003,** *13* (1), 84-94.
37. Potter, M. C.; Figuera-Losada, M.; Rojas, C.; Slusher, B. S., Targeting the glutamatergic system for the treatment of HIV-associated neurocognitive disorders. *J Neuroimmune Pharmacol* **2013,** *8* (3), 594-607.
38. Kovalevich, J.; Langford, D., Neuronal toxicity in HIV CNS disease. *Future virology* **2012,** *7* (7), 687-698.
39. Fontana, A. C., Current approaches to enhance glutamate transporter function and expression. *J Neurochem* **2015,** *134* (6), 982-1007.
40. Danbolt, N. C., Glutamate uptake. *Prog Neurobiol* **2001,** *65* (1), 1-105.
41. Maragakis, N. J.; Dykes-Hoberg, M.; Rothstein, J. D., Altered expression of the glutamate transporter EAAT2b in neurological disease. *Ann Neurol* **2004,** *55* (4), 469-77.
42. Lauriat, T. L.; McInnes, L. A., EAAT2 regulation and splicing: relevance to psychiatric and neurological disorders. *Mol Psychiatry* **2007,** *12* (12), 1065-78.
43. Kim, K.; Lee, S. G.; Kegelman, T. P.; Su, Z. Z.; Das, S. K.; Dash, R.; Dasgupta, S.; Barral, P. M.; Hedvat, M.; Diaz, P.; Reed, J. C.; Stebbins, J. L.; Pellecchia, M.; Sarkar, D.; Fisher, P. B., Role of excitatory amino acid transporter-2 (EAAT2) and glutamate in neurodegeneration: opportunities for developing novel therapeutics. *J Cell Physiol* **2011,** *226* (10), 2484-93.
44. Pines, G.; Danbolt, N. C.; Bjoras, M.; Zhang, Y.; Bendahan, A.; Eide, L.; Koepsell, H.; Storm-Mathisen, J.; Seeberg, E.; Kanner, B. I., Cloning and expression of a rat brain L-glutamate transporter. *Nature* **1992,** *360* (6403), 464-7.
45. Haugeto, O.; Ullensvang, K.; Levy, L. M.; Chaudhry, F. A.; Honore, T.; Nielsen, M.; Lehre, K. P.; Danbolt, N. C., Brain glutamate transporter proteins form homomultimers. *J Biol Chem* **1996,** *271* (44), 27715-22.
46. Gegelashvili, G.; Danbolt, N. C.; Schousboe, A., Neuronal soluble factors differentially regulate the expression of the GLT1 and GLAST glutamate transporters in cultured astroglia. *J Neurochem* **1997,** *69* (6), 2612-5.
47. Gegelashvili, G.; Civenni, G.; Racagni, G.; Danbolt, N. C.; Schousboe, I.; Schousboe, A., Glutamate receptor agonists up-regulate glutamate transporter GLAST in astrocytes. *Neuroreport* **1996,** *8* (1), 261-5.
48. Storck, T.; Schulte, S.; Hofmann, K.; Stoffel, W., Structure, expression, and functional analysis of a Na(+)-dependent glutamate/aspartate transporter from rat brain. *Proc Natl Acad Sci U S A* **1992,** *89* (22), 10955-9.
49. Arriza, J. L.; Fairman, W. A.; Wadiche, J. I.; Murdoch, G. H.; Kavanaugh, M. P.; Amara, S. G., Functional comparisons of three glutamate transporter subtypes cloned from human motor cortex. *J Neurosci* **1994,** *14* (9), 5559-69.
50. Kondo, K.; Hashimoto, H.; Kitanaka, J.; Sawada, M.; Suzumura, A.; Marunouchi, T.; Baba, A., Expression of glutamate transporters in cultured glial cells. *Neurosci Lett* **1995,** *188* (2), 140-2.
51. Zhou, Y.; Danbolt, N. C., GABA and Glutamate Transporters in Brain. *Front Endocrinol (Lausanne)* **2013,** *4* (165), 1-14.

52. Lehre, K. P.; Danbolt, N. C., The number of glutamate transporter subtype molecules at glutamatergic synapses: chemical and stereological quantification in young adult rat brain. *J Neurosci* **1998,** *18* (21), 8751-7.
53. Suchak, S. K.; Baloyianni, N. V.; Perkinton, M. S.; Williams, R. J.; Meldrum, B. S.; Rattray, M., The 'glial' glutamate transporter, EAAT2 (Glt-1) accounts for high affinity glutamate uptake into adult rodent nerve endings. *J Neurochem* **2003,** *84* (3), 522-32.
54. Scofield, M. D.; Kalivas, P. W., Astrocytic dysfunction and addiction: consequences of impaired glutamate homeostasis. *Neuroscientist* **2014,** *20* (6), 610-22.
55. Pajarillo, E.; Rizor, A.; Lee, J.; Aschner, M.; Lee, E., The role of astrocytic glutamate transporters GLT-1 and GLAST in neurological disorders: Potential targets for neurotherapeutics. *Neuropharmacology* **2019,** *161*, 107559-73.
56. Alam, M. A.; Datta, P. K., Epigenetic Regulation of Excitatory Amino Acid Transporter 2 in Neurological Disorders. *Front Pharmacol* **2019,** *10*, 1510.
57. O'Donovan, S. M.; Sullivan, C. R.; McCullumsmith, R. E., The role of glutamate transporters in the pathophysiology of neuropsychiatric disorders. *NPJ Schizophr* **2017,** *3* (32), 1-14.
58. Robinson, M. B.; Jackson, J. G., Astroglial glutamate transporters coordinate excitatory signaling and brain energetics. *Neurochem Int* **2016,** (98), 56-71.
59. Takahashi, K.; Foster, J. B.; Lin, C. L., Glutamate transporter EAAT2: regulation, function, and potential as a therapeutic target for neurological and psychiatric disease. *Cell Mol Life Sci* **2015,** *72* (18), 3489-506.
60. Bjorn-Yoshimoto, W. E.; Underhill, S. M., The importance of the excitatory amino acid transporter 3 (EAAT3). *Neurochem Int* **2016,** *98*, 4-18.
61. Perkins, E. M.; Clarkson, Y. L.; Suminaite, D.; Lyndon, A. R.; Tanaka, K.; Rothstein, J. D.; Skehel, P. A.; Wyllie, D. J. A.; Jackson, M., Loss of cerebellar glutamate transporters EAAT4 and GLAST differentially affects the spontaneous firing pattern and survival of Purkinje cells. *Hum Mol Genet* **2018,** *27* (15), 2614-2627.
62. Tse, D. Y.; Chung, I.; Wu, S. M., Pharmacological inhibitions of glutamate transporters EAAT1 and EAAT2 compromise glutamate transport in photoreceptor to ON-bipolar cell synapses. *Vision Res* **2014,** *103*, 49-62.
63. Jin, X.-T.; Paré, J.-F.; Smith, Y., Differential localization and function of GABA transporters, GAT-1 and GAT-3, in the rat globus pallidus. *The European journal of neuroscience* **2011,** *33* (8), 1504-1518.
64. Krogsgaard-Larsen, P.; Falch, E.; Larsson, O. M.; Schousboe, A., GABA uptake inhibitors: relevance to antiepileptic drug research. *Epilepsy Res* **1987,** *1* (2), 77-93.
65. Dalby, N. O., Inhibition of gamma-aminobutyric acid uptake: anatomy, physiology and effects against epileptic seizures. *Eur J Pharmacol* **2003,** *479* (1-3), 127-37.
66. Walker, M. C., Pathophysiology of status epilepticus. *Neurosci Lett* **2018,** *667*, 84-91.
67. Schousboe, A.; Wellendorph, P.; Frolund, B.; Clausen, R. P.; Krogsgaard-Larsen, P., Astrocytic GABA Transporters: Pharmacological Properties and Targets for Antiepileptic Drugs. *Adv Neurobiol* **2017,** *16*, 283-296.
68. Vandenberg, R. J.; Ryan, R. M.; Carland, J. E.; Imlach, W. L.; Christie, M. J., Glycine transport inhibitors for the treatment of pain. *Trends in Pharmacological Sciences* **2014,** *35* (8), 423-430.

69. Cioffi, C. L.; Guzzo, P. R., Inhibitors of Glycine Transporter-1: Potential Therapeutics for the Treatment of CNS Disorders. *Curr Top Med Chem* **2016,** *16* (29), 3404-3437.
70. Mostyn, S. N.; Wilson, K. A.; Schumann-Gillett, A.; Frangos, Z. J.; Shimmon, S.; Rawling, T.; Ryan, R. M.; O'Mara, M. L.; Vandenberg, R. J., Identification of an allosteric binding site on the human glycine transporter, GlyT2, for bioactive lipid analgesics. *eLife* **2019,** *8* (e47150), 1-22.
71. Fontana, A. C.; de Oliveira Beleboni, R.; Wojewodzic, M. W.; Ferreira Dos Santos, W.; Coutinho-Netto, J.; Grutle, N. J.; Watts, S. D.; Danbolt, N. C.; Amara, S. G., Enhancing glutamate transport: mechanism of action of Parawixin1, a neuroprotective compound from Parawixia bistriata spider venom. *Mol Pharmacol* **2007,** *72* (5), 1228-37.
72. Gelfuso, E. A.; Liberato, J. L.; Cunha, A. O.; Mortari, M. R.; Beleboni, R. O.; Lopes, N. P.; Dos Santos, W. F., Parawixin2, a novel non-selective GABA uptake inhibitor from Parawixia bistriata spider venom, inhibits pentylenetetrazole-induced chemical kindling in rats. *Neurosci Lett* **2013,** *543*, 12-6.
73. Beleboni, R.; Guizzo, R.; Fontana, A.; Pizzo, A.; Carolino, R.; Gobbo-Neto, L.; Lopes, N.; Coutinho-Netto, J.; dos Santos, W., Neurochemical characterization of a neuroprotective compound from Parawixia bistriata spider venom that inhibits synaptosomal uptake of GABA and glycine. *Molecular Pharmacology* **2006,** *69* (6), 1998-2006.
74. Gelfuso, E. A.; Cunha, A. O.; Mortari, M. R.; Liberato, J. L.; Paraventi, K. H.; Beleboni, R. O.; Coutinho-Netto, J.; Lopes, N. P.; dos Santos, W. F., Neuropharmacological profile of FrPbAII, purified from the venom of the social spider Parawixia bistriata (Araneae, Araneidae), in Wistar rats. *Life Sci* **2007,** *80* (6), 566-72.
75. Liberato, J. L.; Godoy, L. D.; Cunha, A. O. S.; Mortari, M. R.; de Oliveira Beleboni, R.; Fontana, A. C. K.; Lopes, N. P.; Dos Santos, W. F., Parawixin2 Protects Hippocampal Cells in Experimental Temporal Lobe Epilepsy. *Toxins (Basel)* **2018,** *10* (12), 1-27.
76. Godoy, L. D.; Liberato, J. L.; Celani, M. V. B.; Gobbo-Neto, L.; Lopes, N. P.; Dos Santos, W. F., Disease Modifying Effects of the Spider Toxin Parawixin2 in the Experimental Epilepsy Model. *Toxins (Basel)* **2017,** *9* (9), 1-19.
77. Liberato, J. L.; Cunha, A. O.; Mortari, M. R.; Gelfuso, E. A.; Beleboni Rde, O.; Coutinho-Netto, J.; dos Santos, W. F., Anticonvulsant and anxiolytic activity of FrPbAII, a novel GABA uptake inhibitor isolated from the venom of the social spider Parawixia bistriata (Araneidae: Araneae). *Brain Res* **2006,** *1124* (1), 19-27.
78. Fachim, H. A.; Cunha, A. O.; Pereira, A. C.; Beleboni, R. O.; Gobbo-Neto, L.; Lopes, N. P.; Coutinho-Netto, J.; dos Santos, W. F., Neurobiological activity of Parawixin 10, a novel anticonvulsant compound isolated from Parawixia bistriata spider venom (Araneidae: Araneae). *Epilepsy Behav* **2011,** *22* (2), 158-64.
79. Fachim, H. A.; Mortari, M. R.; Gobbo-Netto, L.; Dos Santos, W. F., Neuroprotective activity of parawixin 10, a compound isolated from Parawixia bistriata spider venom (Araneidae: Araneae) in rats undergoing intrahippocampal NMDA microinjection. *Pharmacogn Mag* **2015,** *11* (43), 579-85.
80. Mortensen, O. V.; Liberato, J. L.; Coutinho-Netto, J.; Dos Santos, W. F.; Fontana, A. C., Molecular determinants of transport stimulation of EAAT2 are located at interface between the trimerization and substrate transport domains. *J Neurochem* **2015,** *133* (2), 199-210.

81. Kortagere, S.; Mortensen, O. V.; Xia, J.; Lester, W.; Fang, Y.; Srikanth, Y.; Salvino, J. M.; Fontana, A. C. K., Identification of Novel Allosteric Modulators of Glutamate Transporter EAAT2. *ACS Chem Neurosci* **2018,** *9* (3), 522-534.
82. Falcucci, R. M.; Wertz, R.; Green, J. L.; Meucci, O.; Salvino, J.; Fontana, A. C. K., Novel Positive Allosteric Modulators of Glutamate Transport Have Neuroprotective Properties in an in Vitro Excitotoxic Model. *ACS Chem Neurosci* **2019,** *10* (8), 3437-3453.
83. Tzouros, M.; Chesnov, S.; Bigler, L.; Bienz, S., A template approach for the characterization of linear polyamines and derivatives in spider venom. *Eur J Mass Spectrom (Chichester, Eng)* **2013,** *19* (1), 57-69.
84. Tzouros, M.; Manov, N.; Bienz, S.; Bigler, L., Tandem mass spectrometric investigation of acylpolyamines of spider venoms and their 15N-labeled derivatives. *J Am Soc Mass Spectrom* **2004,** *15* (11), 1636-43.
85. Rodrigues, M. C.; Guizzo, R.; Gobbo-Neto, L.; Ward, R. J.; Lopes, N. P.; dos Santos, W. F., The biological activity in mammals and insects of the nucleosidic fraction from the spider Parawixia bistriata. *Toxicon* **2004,** *43* (4), 375-83.
86. Chan, T. K.; Geren, C. R.; Howell, D. E.; Odell, G. V., Adenosine triphosphate in tarantula spider venoms and its synergistic effect with the venom toxin. *Toxicon* **1975,** *13* (1), 61-66.
87. Horni, A.; Weickmann, D.; Hesse, M., The main products of the low molecular mass fraction in the venom of the spider Latrodectus menavodi. *Toxicon* **2001,** *39* (2-3), 425-8.
88. Schroeder, F. C.; Taggi, A. E.; Gronquist, M.; Malik, R. U.; Grant, J. B.; Eisner, T.; Meinwald, J., NMR-spectroscopic screening of spider venom reveals sulfated nucleosides as major components for the brown recluse and related species. *Proc Natl Acad Sci U S A* **2008,** *105* (38), 14283-7.
89. Moore, S.; Smyth, W. F.; Gault, V. A.; O'Kane, E.; McClean, S., Mass spectrometric characterisation and quantitation of selected low molecular mass compounds from the venom of Haplopelma lividum (Theraphosidae). *Rapid Commun Mass Spectrom* **2009,** *23* (12), 1747-55.
90. Kuhn-Nentwig, L.; Schaller, J.; Nentwig, W., Purification of toxic peptides and the amino acid sequence of CSTX-1 from the multicomponent venom of Cupiennius salei (Araneae:Ctenidae). *Toxicon* **1994,** *32* (3), 287-302.
91. Kuhn-Nentwig, L.; Stöcklin, R.; Nentwig, W., Venom Composition and Strategies in Spiders: Is Everything Possible?☆☆Dedicated to Prof. Dr. Lev G. Magazanik, Sechenov Institute of Evolutionary Physiology and Biochemistry, RAS, St. Petersburg, Russia, at the occasion of his 80th anniversary. In *Advances in Insect Physiology*, Casas, J., Ed. Academic Press: 2011; Vol. 40, pp 1-86.
92. Usherwood, P. N.; Duce, I. R.; Boden, P., Slowly-reversible block of glutamate receptor-channels by venoms of the spiders, Argiope trifasciata and Araneus gemma. *J Physiol (Paris)* **1984,** *79* (4), 241-5.
93. Adams, M. E.; Carney, R. L.; Enderlin, F. E.; Fu, E. T.; Jarema, M. A.; Li, J. P.; Miller, C. A.; Schooley, D. A.; Shapiro, M. J.; Venema, V. J., Structures and biological activities of three synaptic antagonists from orb weaver spider venom. *Biochem Biophys Res Commun* **1987,** *148* (2), 678-83.
94. Budd, T.; Clinton, P.; Dell, A.; Duce, I. R.; Johnson, S. J.; Quicke, D. L. J.; Taylor, G. W.; Usherwood, P. N. R.; Usoh, G., Isolation and characterisation of glutamate receptor antagonists from venoms of orb-web spiders. *Brain Research* **1988,** *448* (1), 30-39.

95. Cesar, L. M. M.; Tormena, C. F.; Marques, M. R.; Silva, G. V. J.; Mendes, M. A.; Rittner, R.; Palma, M. S., Structure Determination of Hydroxytrypargine: A New Tetrahydro-β-Carboline Toxin from the Venom of the Spider Parawixia bistriata. *Helvetica Chimica Acta* **2005,** *88* (4), 796-801.
96. Cesar, L. M.; Mendes, M. A.; Tormena, C. F.; Marques, M. R.; de Souza, B. M.; Saidemberg, D. M.; Bittencourt, J. C.; Palma, M. S., Isolation and chemical characterization of PwTx-II: a novel alkaloid toxin from the venom of the spider Parawixia bistriata (Araneidae, Araneae). *Toxicon* **2005,** *46* (7), 786-96.
97. Saidemberg, D. M.; Ferreira, M. A.; Takahashi, T. N.; Gomes, P. C.; Cesar-Tognoli, L. M.; da Silva-Filho, L. C.; Tormena, C. F.; da Silva, G. V.; Palma, M. S., Monoamine oxidase inhibitory activities of indolylalkaloid toxins from the venom of the colonial spider Parawixia bistriata: functional characterization of PwTX-I. *Toxicon* **2009,** *54* (6), 717-24.
98. Krause, S.; Schwarz, W., Identification and selective inhibition of the channel mode of the neuronal GABA transporter 1. *Mol Pharmacol* **2005,** *68* (6), 1728-35.
99. Laughlin, T. M.; Tram, K. V.; Wilcox, G. L.; Birnbaum, A. K., Comparison of antiepileptic drugs tiagabine, lamotrigine, and gabapentin in mouse models of acute, prolonged, and chronic nociception. *J Pharmacol Exp Ther* **2002,** *302* (3), 1168-75.
100. Damgaard, M.; Al-Khawaja, A.; Vogensen, S. B.; Jurik, A.; Sijm, M.; Lie, M. E.; Baek, M. I.; Rosenthal, E.; Jensen, A. A.; Ecker, G. F.; Frolund, B.; Wellendorph, P.; Clausen, R. P., Identification of the First Highly Subtype-Selective Inhibitor of Human GABA Transporter GAT3. *ACS Chem Neurosci* **2015,** *6* (9), 1591-9.
101. Schousboe, A.; Madsen, K. K.; Barker-Haliski, M. L.; White, H. S., The GABA synapse as a target for antiepileptic drugs: a historical overview focused on GABA transporters. *Neurochem Res* **2014,** *39* (10), 1980-7.
102. Grishin, E. V.; Volkova, T. M.; Arseniev, A. S., Isolation and structure analysis of components from venom of the spider Argiope lobata. *Toxicon* **1989,** *27* (5), 541-9.
103. Yamaji, N.; Horikawa, M.; Corzo, G.; Naoki, H.; Haupt, J.; Nakajima, T.; Iwashita, T., Structure and enantioselective synthesis of polyamine toxin MG30 from the venom of the spider Macrothele gigas. *Tetrahedron Letters* **2004,** *45* (28), 5371-5373.
104. Eichenberger, S. Development of a high-resolution MS-based method for the structural elucidation of polyamine spider toxins. University of Zurich Main Library, Zurich Open Repository and Archive, 2009. https://doi.org/10.5167/uzh-12787.
105. Wakamiya, T.; Kinoshita, T.; Hattori, Y.; Yamaguchi, Y.; Naoki, H.; Corzo, G.; Nakajima, T., Study on the Structure Activity Relationships of NPTX-594, a Spider Toxin Belonging to the Type-B Acylpolyamine Structure. *Bulletin of the Chemical Society of Japan* **2004,** *77* (2), 331-340.
106. Tateaki, W.; Akinori, Y.; Keita, K.; Tomohiko, K.; Yoshihiro, Y.; Yasuhiro, I.; Hideo, N.; Terumi, N., Total Synthesis of the Novel Spider Toxin NPTX-594 from Nephila madagascariencis. *Bulletin of the Chemical Society of Japan* **2001,** *74* (9), 1743-1749.
107. Toki, T.; Yasuhara, T.; Aramaki, Y.; Osawa, K.; Miwa, A.; Kawai, N.; Nakajima, T., ISOLATION AND CHEMICAL CHARACTERIZATION OF A SERIES OF NEW SPIDER TOXIN (NEPHILATOXINS) IN THE VENOM OF JORO SPIDER, *NEPHILA CLAVATA Biomedical Research* **1988,** *9* (6), 421-428.
108. Pereira, L. S.; Silva, P. I., Jr.; Miranda, M. T.; Almeida, I. C.; Naoki, H.; Konno, K.; Daffre, S., Structural and biological characterization of one antibacterial acylpolyamine isolated from the hemocytes of the spider Acanthocurria gomesiana. *Biochem Biophys Res Commun* **2007,** *352* (4), 953-9.

109. Wilson, D.; Boyle, G. M.; McIntyre, L.; Nolan, M. J.; Parsons, P. G.; Smith, J. J.; Tribolet, L.; Loukas, A.; Liddell, M. J.; Rash, L. D.; Daly, N. L., The Aromatic Head Group of Spider Toxin Polyamines Influences Toxicity to Cancer Cells. *Toxins (Basel)* **2017,** *9* (11), 1-13.
110. Akyuz, N.; Georgieva, E. R.; Zhou, Z.; Stolzenberg, S.; Cuendet, M. A.; Khelashvili, G.; Altman, R. B.; Terry, D. S.; Freed, J. H.; Weinstein, H.; Boudker, O.; Blanchard, S. C., Transport domain unlocking sets the uptake rate of an aspartate transporter. *Nature* **2015,** *518* (7537), 68-73.
111. Akyuz, N.; Altman, R. B.; Blanchard, S. C.; Boudker, O., Transport dynamics in a glutamate transporter homologue. *Nature* **2013,** *502* (7469), 114-8.
112. Reyes, N.; Ginter, C.; Boudker, O., Transport mechanism of a bacterial homologue of glutamate transporters. *Nature* **2009,** *462* (7275), 880-5.
113. Canul-Tec, J. C.; Assal, R.; Cirri, E.; Legrand, P.; Brier, S.; Chamot-Rooke, J.; Reyes, N., Structure and allosteric inhibition of excitatory amino acid transporter 1. *Nature* **2017,** *544* (7651), 446-451.
114. Menniti, F. S.; Lindsley, C. W.; Conn, P. J.; Pandit, J.; Zagouras, P.; Volkmann, R. A., Allosteric modulators for the treatment of schizophrenia: targeting glutamatergic networks. *Current topics in medicinal chemistry* **2013,** *13* (1), 26-54.
115. Usherwood, P. N. R.; Blagbrough, I. S., Spider toxins affecting glutamate receptors: Polyamines in therapeutic neurochemistry. *Pharmacology & Therapeutics* **1991,** *52* (2), 245-268.
116. Xiong, X. F.; Poulsen, M. H.; Hussein, R. A.; Norager, N. G.; Stromgaard, K., Structure-activity relationship study of spider polyamine toxins as inhibitors of ionotropic glutamate receptors. *ChemMedChem* **2014,** *9* (12), 2661-70.
117. Chernova, T.; Steinert, J. R.; Guerin, C. J.; Nicotera, P.; Forsythe, I. D.; Smith, A. G., Neurite Degeneration Induced by Heme Deficiency Mediated via Inhibition of NMDA Receptor-Dependent Extracellular Signal-Regulated Kinase 1/2 Activation. *The Journal of Neuroscience* **2007,** *27* (32), 8475-8485.
118. Nicolai, J.; Burbassi, S.; Rubin, J.; Meucci, O., CXCL12 inhibits expression of the NMDA receptor's NR2B subunit through a histone deacetylase-dependent pathway contributing to neuronal survival. *Cell Death Dis* **2010,** *1*, e33.
119. Hardingham, G. E.; Bading, H., Synaptic versus extrasynaptic NMDA receptor signalling: implications for neurodegenerative disorders. *Nat Rev Neurosci* **2010,** *11* (10), 682-96.
120. Arundine, M.; Tymianski, M., Molecular mechanisms of glutamate-dependent neurodegeneration in ischemia and traumatic brain injury. *Cell Mol Life Sci* **2004,** *61* (6), 657-68.
121. Lewerenz, J.; Maher, P., Chronic Glutamate Toxicity in Neurodegenerative Diseases-What is the Evidence? *Front Neurosci* **2015,** *9*, 469.
122. Phillis, J. W.; Ren, J.; O'Regan, M. H., Transporter reversal as a mechanism of glutamate release from the ischemic rat cerebral cortex: studies with DL-threo-beta-benzyloxyaspartate. *Brain Res* **2000,** *880* (1-2), 224.
123. Kosugi, T.; Kawahara, K., Reversed actrocytic GLT-1 during ischemia is crucial to excitotoxic death of neurons, but contributes to the survival of astrocytes themselves. *Neurochem Res* **2006,** *31* (7), 933-43.
124. Hurtado, O.; Moro, M. A.; Cárdenas, A.; Sánchez, V.; Fernández-Tomé, P.; Leza, J. C.; Lorenzo, P.; Secades, J. J.; Lozano, R.; Dávalos, A.; Castillo, J.; Lizasoain, I., Neuroprotection afforded by prior citicoline administration in experimental brain ischemia: effects on glutamate transport. *Neurobiology of Disease* **2005,** *18* (2), 336-345.

125. Verma, R.; Mishra, V.; Sasmal, D.; Raghubir, R., Pharmacological evaluation of glutamate transporter 1 (GLT-1) mediated neuroprotection following cerebral ischemia/reperfusion injury. *Eur J Pharmacol* **2010,** *638* (1-3), 65-71.
126. Chao, X. D.; Fei, F.; Fei, Z., The role of excitatory amino acid transporters in cerebral ischemia. *Neurochem Res* **2010,** *35* (8), 1224-30.
127. Krzyzanowska, W.; Pomierny, B.; Bystrowska, B.; Pomierny-Chamiolo, L.; Filip, M.; Budziszewska, B.; Pera, J., Ceftriaxone- and N-acetylcysteine-induced brain tolerance to ischemia: Influence on glutamate levels in focal cerebral ischemia. *PLoS One* **2017,** *12* (10), e0186243.
128. Krzyzanowska, W.; Pomierny, B.; Filip, M.; Pera, J., Glutamate transporters in brain ischemia: to modulate or not? *Acta Pharmacol Sin* **2014,** *35* (4), 444-62.
129. Niswender, C. M.; Conn, P. J., Metabotropic Glutamate Receptors: Physiology, Pharmacology, and Disease. *Annual review of pharmacology and toxicology* **2010,** *50*, 295-322.
130. von Bartheld, C. S.; Bahney, J.; Herculano-Houzel, S., The search for true numbers of neurons and glial cells in the human brain: A review of 150 years of cell counting. *J Comp Neurol* **2016,** *524* (18), 3865-3895.
131. Chaudhry, F. A.; Reimer, R. J.; Edwards, R. H., The glutamine commute: take the N line and transfer to the A. *J Cell Biol* **2002,** *157* (3), 349-55.
132. Hertz, L.; Chen, Y., Integration between Glycolysis and Glutamate-Glutamine Cycle Flux May Explain Preferential Glycolytic Increase during Brain Activation, Requiring Glutamate. *Front Integr Neurosci* **2017,** *11*, 18.
133. Jong, Y.-J. I.; O'Malley, K. L., Mechanisms Associated with Activation of Intracellular Metabotropic Glutamate Receptor, mGluR5. *Neurochemical Research* **2017,** *42* (1), 166-172.
134. Jong, Y.-J. I.; Kumar, V.; O'Malley, K. L., Intracellular Metabotropic Glutamate Receptor 5 (mGluR5) Activates Signaling Cascades Distinct from Cell Surface Counterparts. *The Journal of Biological Chemistry* **2009,** *284* (51), 35827-35838.
135. Szafran, M.; Koput, J.; Dega-Szafran, Z.; Katrusiak, A., X-ray and ab initio studies of the structure and vibrational spectra of 4-carboxy-1-methylpyridinium chloride. *Journal of Molecular Structure* **2006,** *797* (1), 66-81.
136. Timple, J. M. V.; Magalhaes, L. G.; Souza Rezende, K. C.; Pereira, A. C.; Cunha, W. R.; Andrade e Silva, M. L.; Mortensen, O. V.; Fontana, A. C. K., The Lignan (-)-Hinokinin Displays Modulatory Effects on Human Monoamine and GABA Transporter Activities. *Journal of Natural Products* **2013,** *76* (10), 1889-1895.
137. Yoshikawa, K., Cell cycle regulators in neural stem cells and postmitotic neurons. *Neurosci Res* **2000,** *37* (1), 1-14.
138. Guillet, B.; Lortet, S.; Masmejean, F.; Samuel, D.; Nieoullon, A.; Pisano, P., Developmental expression and activity of high affinity glutamate transporters in rat cortical primary cultures. *Neurochemistry International* **2002,** *40* (7), 661-671.
139. Plachez, C.; Danbolt, N. C.; Recasens, M., Transient expression of the glial glutamate transporters GLAST and GLT in hippocampal neurons in primary culture. *J Neurosci Res* **2000,** *59* (5), 587-93.
140. Cook, A.; Hippensteel, R.; Shimizu, S.; Nicolai, J.; Fatatis, A.; Meucci, O., Interactions between chemokines: regulation of fractalkine/CX3CL1 homeostasis by SDF/CXCL12 in cortical neurons. *J Biol Chem* **2010,** *285* (14), 10563-71.
141. Meucci, O.; Fatatis, A.; Simen, A. A.; Bushell, T. J.; Gray, P. W.; Miller, R. J., Chemokines regulate hippocampal neuronal signaling and gp120 neurotoxicity. *Proc Natl Acad Sci U S A* **1998,** *95* (24), 14500-5.

142. O'Donnell, L. A.; Agrawal, A.; Jordan-Sciutto, K. L.; Dichter, M. A.; Lynch, D. R.; Kolson, D. L., Human immunodeficiency virus (HIV)-induced neurotoxicity: roles for the NMDA receptor subtypes. *J Neurosci* **2006,** *26* (3), 981-90.
143. Holloway, P. M.; Gavins, F. N. E., Modeling Ischemic Stroke In Vitro: Status Quo and Future Perspectives. *Stroke* **2016,** *47* (2), 561-569.
144. Cook, D. R.; Gleichman, A. J.; Cross, S. A.; Doshi, S.; Ho, W.; Jordan-Sciutto, K. L.; Lynch, D. R.; Kolson, D. L., NMDA receptor modulation by the neuropeptide apelin: implications for excitotoxic injury. *J Neurochem* **2011,** *118* (6), 1113-23.
145. Wang, Y.; White, M. G.; Akay, C.; Chodroff, R. A.; Robinson, J.; Lindl, K. A.; Dichter, M. A.; Qian, Y.; Mao, Z.; Kolson, D. L.; Jordan-Sciutto, K. L., Activation of cyclin-dependent kinase 5 by calpains contributes to human immunodeficiency virus-induced neurotoxicity. *J Neurochem* **2007,** *103* (2), 439-55.
146. White, M. G.; Wang, Y.; Akay, C.; Lindl, K. A.; Kolson, D. L.; Jordan-Sciutto, K. L., Parallel high throughput neuronal toxicity assays demonstrate uncoupling between loss of mitochondrial membrane potential and neuronal damage in a model of HIV-induced neurodegeneration. *Neurosci Res* **2011,** *70* (2), 220-9.
147. Nakajima, Y.; Iguchi, H.; Kamisuki, S.; Sugawara, F.; Furuichi, T.; Shinoda, Y., Low doses of the mycotoxin citrinin protect cortical neurons against glutamate-induced excitotoxicity. *J Toxicol Sci* **2016,** *41* (2), 311-9.

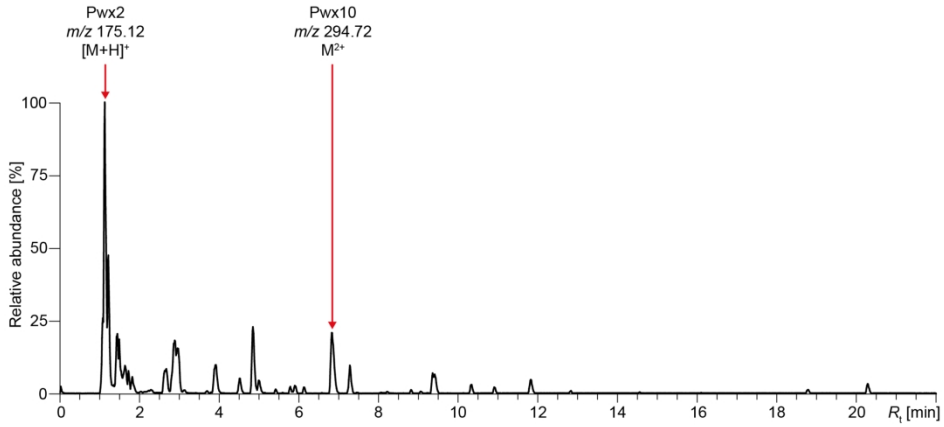

Figure 1: Base peak chromatogram (BPC) of the *P. bistriata* venom with indication of the peaks related to previously isolated neuroprotective fractions Pwx2 and Pwx10.

208x119mm (300 x 300 DPI)

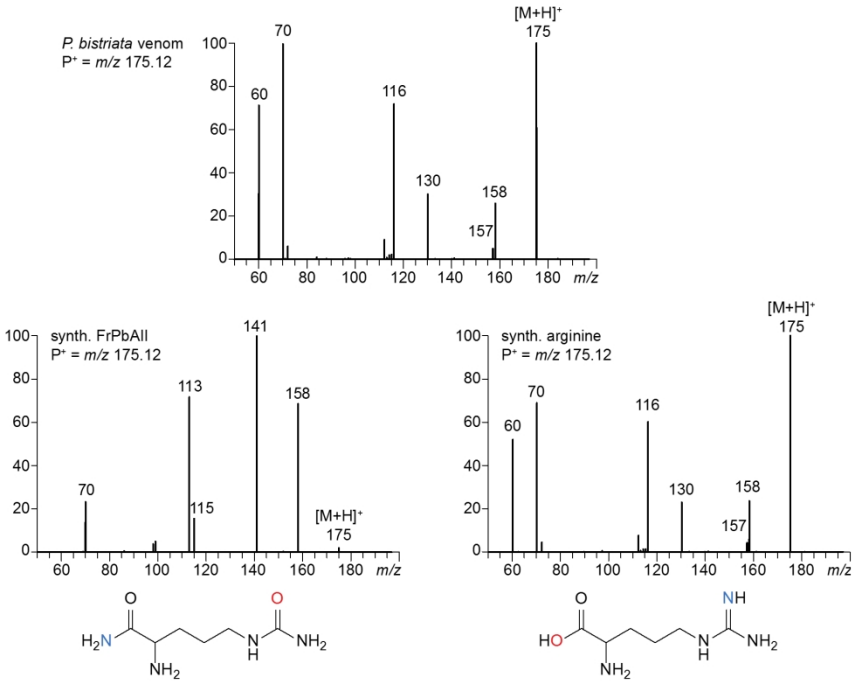

Figure 2: The MS/MS spectrum of the precursor ion m/z 175.12 [M+H]+ found in the crude venom of *P. bistriata* (top) compared to the MS/MS spectra recorded from the commercial reference material FrPbAII (left) and arginine (right) proving that the spider venom contains in fact arginine but not FrPbAII.

186x143mm (300 x 300 DPI)

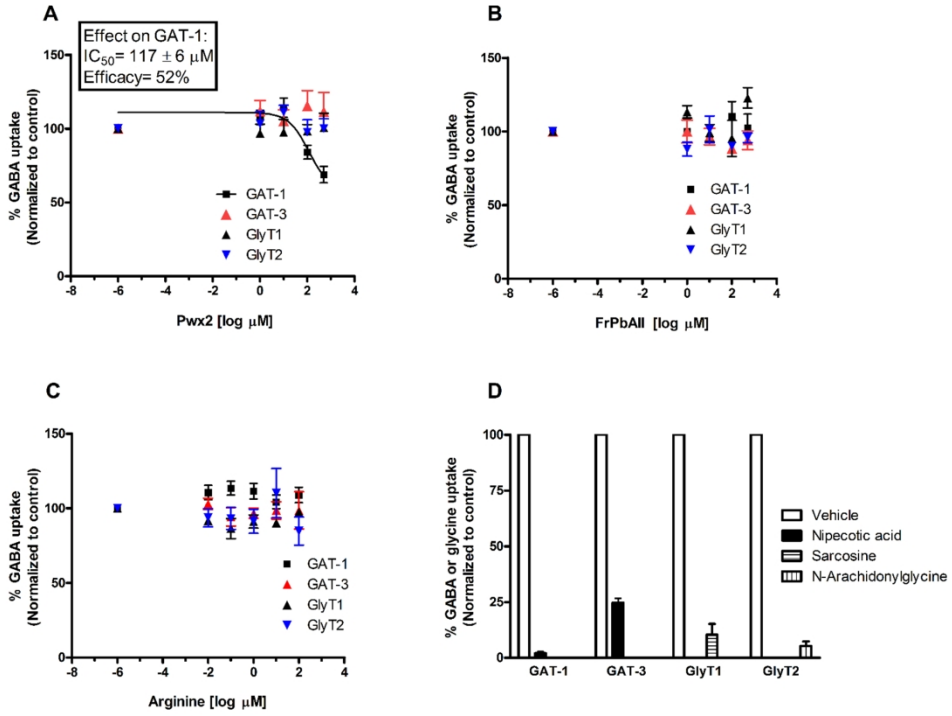

Figure 3: Uptake assays in COS-7 cells transfected with GABA transporters GAT-1 and GAT-3 and glycine transporters GlyT1 and GlyT2 reveal that natural fraction Pwx2 inhibits GABA uptake specifically through GAT-1. A. Dose-response curves of Pwx2 fraction, B. Dose response curves of commercial FrPbAII, C. Dose-response curves of arginine, D. Effects of nipecotic acid (1 mM) on both GAT-1 and GAT-3 transporters and specific GlyT1 inhibitor sarcosine and GlyT2 inhibitor N-Arachidonyl-glycine (100 µM) on glycine transporters. COS-7 cells transiently transfected with appropriate cDNA or empty vector were pre-incubated for 10 min with varied concentrations of compounds and reactions with 50 nM of ^{3}H-GABA or ^{3}H-glycine were carried out for 10 min. Results are normalized to percentage of control (vehicle) and expressed as mean ± SEM of three independent experiments.

183x135mm (300 x 300 DPI)

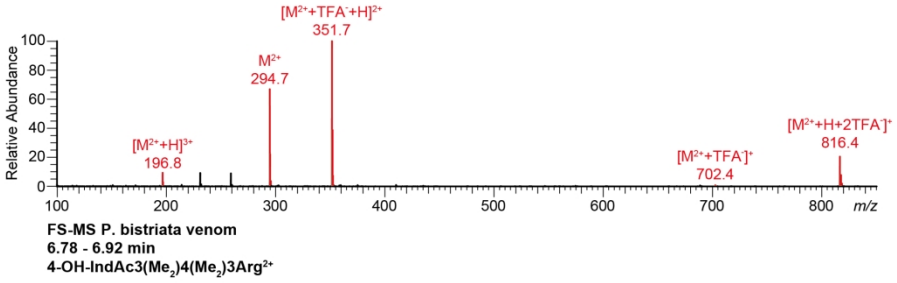

Figure 4: Full scan (FS)-MS of the peak in the UHPLC-MS chromatogram of the *P. bistriata* crude venom (6.78 – 6.92 min), which corresponds to the doubly charged ion m/z 294.7 (main signal detected for the Pwx10 fraction).

210x80mm (300 x 300 DPI)

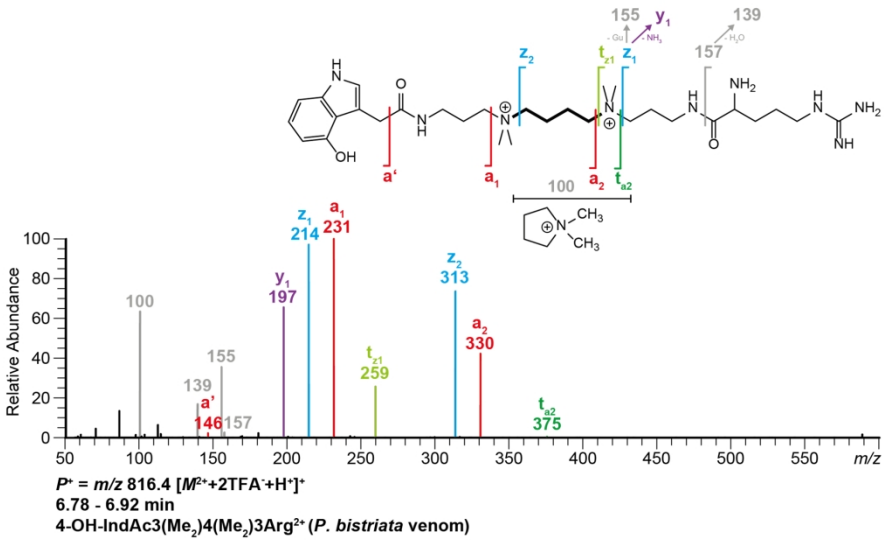

Figure 5: The acylpolyamine 4-OH-IndAc3(Me_2)4(Me_2)3Arg^{2+}; identified from the MS/MS spectrum of the precursor ion m/z 816.4 with fragment ion annotation.

190x119mm (300 x 300 DPI)

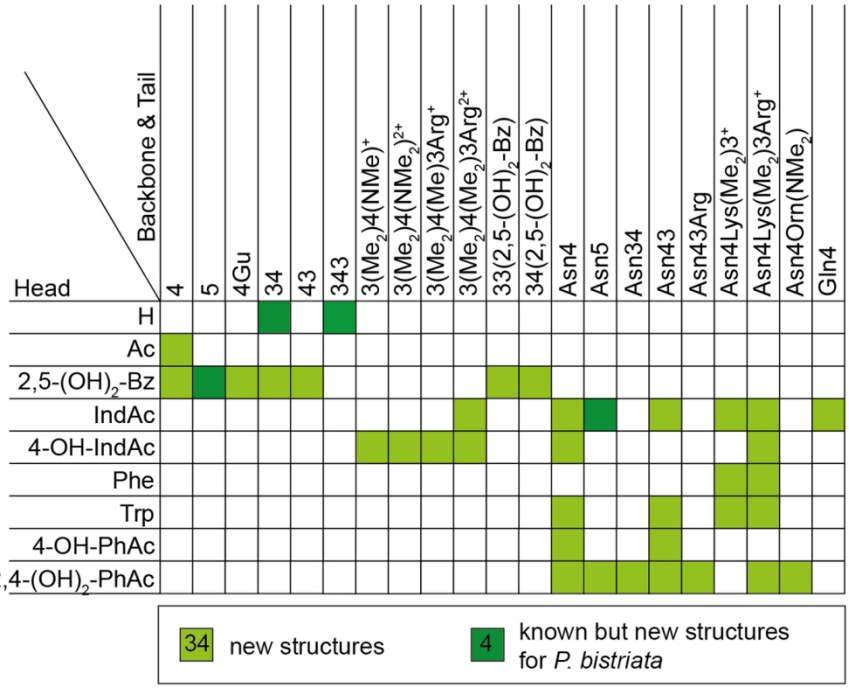

Figure 6: Schematic overview for the free polyamines and acylpolyamines found in the venom of *P. bistriata*. For nomenclature and structures please see supplementary material.

137x109mm (300 x 300 DPI)

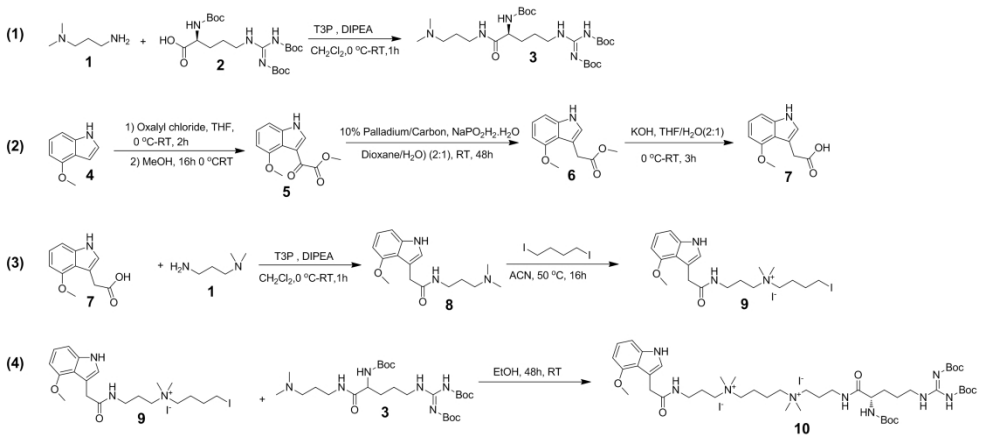

Scheme 1: Synthesis scheme leading to 4-OH-IndAc3(Me_2)4(Me_2)3Arg^{2+}; (shown as compound **12**).

261x122mm (300 x 300 DPI)

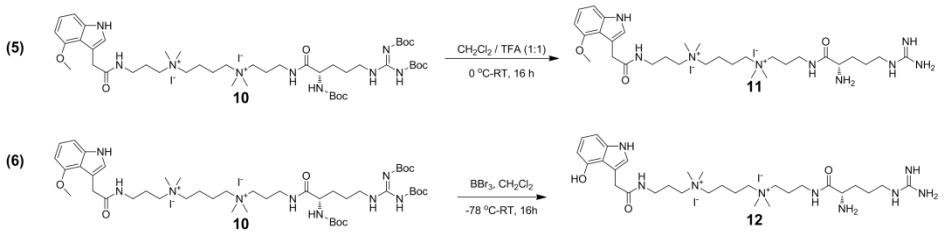

Scheme 2: Synthesis scheme of 4-OH-IndAc3(Me_2)4(Me_2)3Arg^{2+}; (compound **12**).

267x71mm (300 x 300 DPI)

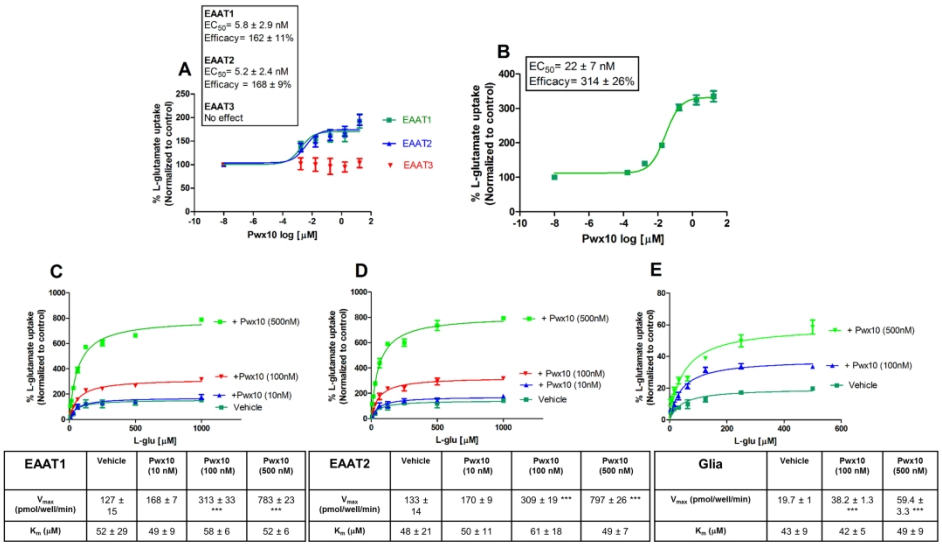

EAAT1	Vehicle	Pwx10 (10 nM)	Pwx10 (100 nM)	Pwx10 (500 nM)
V_{max} (pmol/well/min)	127 ± 15	168 ± 7	313 ± 33 ***	783 ± 23 ***
K_m (µM)	52 ± 29	49 ± 9	58 ± 6	52 ± 6

EAAT2	Vehicle	Pwx10 (10 nM)	Pwx10 (100 nM)	Pwx10 (500 nM)
V_{max} (pmol/well/min)	133 ± 14	170 ± 9	309 ± 19 ***	797 ± 26 ***
K_m (µM)	48 ± 21	50 ± 11	61 ± 18	49 ± 7

Glia	Vehicle	Pwx10 (100 nM)	Pwx10 (500 nM)
V_{max} (pmol/well/min)	19.7 ± 1	38.2 ± 1.3 ***	59.4 ± 3.3 ***
K_m (µM)	43 ± 9	42 ± 5	49 ± 9

Figure 7: Fraction Pwx10 stimulates both EAAT1 and EAAT2-mediated transport. A. Dose response of Pwx10 fraction on L-glutamate transport mediated by EAAT1, EAAT2 or EAAT3 shows that the compound does not modulate EAAT3-mediated transport, but increases EAAT1 and EAAT2; EC_{50s} and efficacies are indicated. Cells were incubated with varied concentrations of compound for 10 min at 37 ^{o}C and 10 min with 50 nM ^{3}H-L-glutamate. Results are normalized to percentage of control (vehicle) and expressed as mean ± SD of three independent experiments, B. Pwx10 fraction augments L-glutamate uptake in a native environment of culture astrocytes. Cells were incubated with varied concentrations of compound for 10 min at 37 ^{o}C and 10 min with 50 nM ^{3}H-L-glutamate. Results are normalized to percentage of control (vehicle) and expressed as Mean ± SD of all the experiments, C. Effects of Pwx10 fraction (10, 100 and 500 nM) on the kinetics of EAAT1, and D. Effects of Pwx10 fraction (10, 100 and 500 nM) on the kinetics of EAAT2. V_{max} and K_M were calculated, and the values are presented in the table; K_M was not statistically different between the varying concentrations of compounds analysed in this study, *** $p < 0.001$, V_{max} comparing compound (100 and 500 nM) to vehicle. Assays were performed in COS-7 cells transiently transfected with appropriate cDNA or empty vector, E. Kinetic analysis of L-glutamate uptake in cultured glia cells pre-incubated with vehicle, 100 nM and 500 nM of Pwx10 fraction. V_{max} and K_M were calculated, and values are presented in the table; K_M was not statistically different between treatments, ***$p < 0.001$, V_{max} comparing compound to vehicle.

296x170mm (300 x 300 DPI)

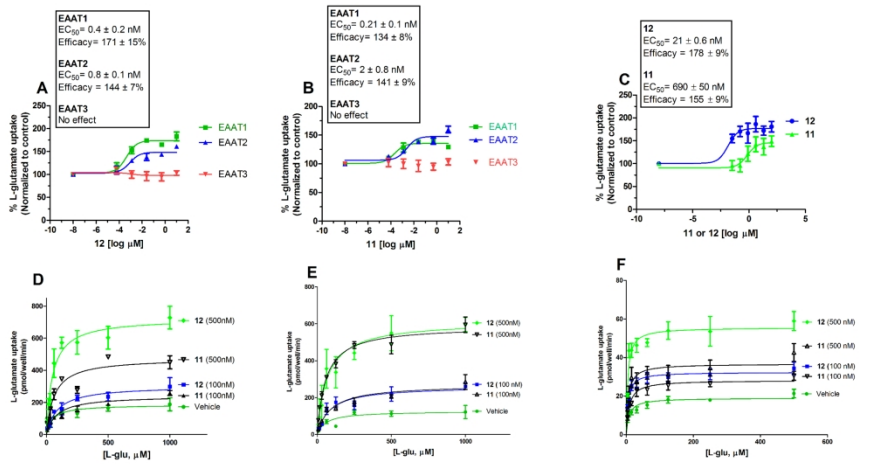

EAAT1	Vehicle	12 (100 nM)	12 (500 nM)	11 (100 nM)	11 (500 nM)
V_{max} (pmol/well/min)	185 ± 15	303 ± 26 **	723 ± 44 ***	241 ± 22 **	475 ± 27 ***
K_m (µM)	49 ± 15	88 ± 25	49 ± 11	52 ± 6	62 ± 14

EAAT2	Vehicle	12 (100 nM)	12 (500 nM)	11 (100 nM)	11 (500 nM)
V_{max} (pmol/well/min)	127 ± 12	262 ± 22 ***	613 ± 55 ***	271 ± 19 ***	586 ± 22 ***
K_m (µM)	59 ± 19	84 ± 24	68 ± 23	89 ± 22	56 ± 8

Glia	Vehicle	12 (100 nM)	12 (500 nM)	11 (100 nM)	11 (500 nM)
V_{max} (pmol/well/min)	18 ± 1	33 ± 2 ***	55 ± 2 ***	28 ± 1 ***	37 ± 2 ***
K_m (µM)	7 ± 2	8 ± 2	4 ± 1	8 ± 1	6 ± 2

Figure 8: Compounds 11 and 12 have similar activities to fraction Pwx10, modulating EAAT1 and EAAT2 transporter activities. Dose responses of **12** (A) and **11** (B) on L-glutamate transport mediated by EAAT1, EAAT2 or EAAT3 shows that the compounds do not modulate EAAT3-mediated transport, but increase EAAT1 and EAAT2; EC_{50s} and efficacies are indicated. Cells were incubated with varied concentrations of compound for 10 min at 37 ^{o}C and 10 min with 50 nM ^{3}H-L-glutamate. Results are normalized to percentage of control (vehicle) and expressed as mean ± SD of three independent experiments, C. **12** and **11** augment L-glutamate uptake in a native environment of culture astrocytes. Cells were incubated with varied concentrations of compounds for 10 min at 37 ^{o}C and 10 min with 50 nM ^{3}H-L-glutamate. Results are normalized to percentage of control (vehicle) and expressed as Mean ± SD of all the experiments, D. Effects of **12** and **11** (100 and 500 nM) on the kinetics of EAAT1, and E. Effects of **12** and **11** (100 and 500 nM) on the kinetics of EAAT2. V_{max} and K_M were calculated, and the values are presented in the table; K_M was not statistically different between the varying concentrations of compounds analysed in this study, *** $p <$ 0.001, V_{max} comparing compound (100 and 500 nM) to vehicle. Assays were performed in COS-7 cells transiently transfected with appropriate cDNA or empty vector, F. Kinetic analysis of L-glutamate uptake in cultured glia cells pre-incubated with vehicle, 100 nM and 500 nM of **12** and **11**. V_{max} and K_M were calculated, and values are presented in the table; K_M was not statistically different between treatments, ***$p <$ 0.001, V_{max} comparing compound to vehicle.

298x190mm (300 x 300 DPI)

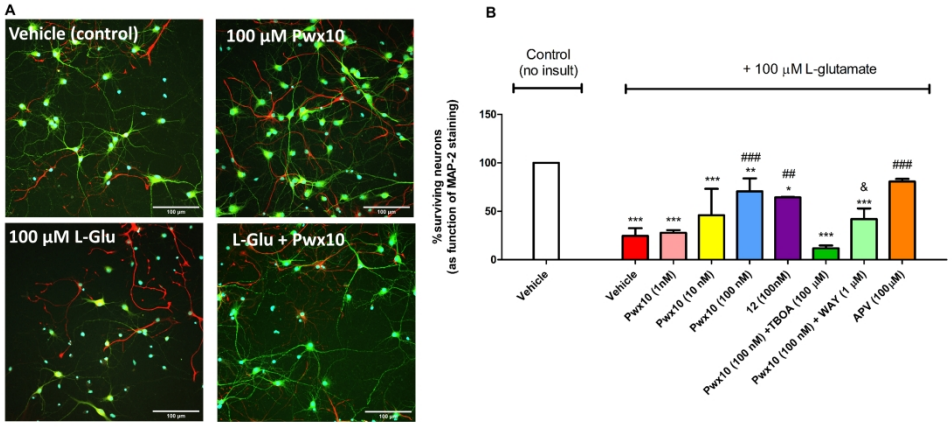

Figure 9: Neuroprotective properties of Pwx10 fraction and 4-OH-IndAc3(Me_2)4(Me_2)3Arg^{2+} (**12**) in mixed neuron-glia cultures after prolonged exposure to L-glutamate. A. Representative Images of 14 DIV mixed neuron-glia cultures in control conditions, after treatments with 100 µM Pwx10 fraction or 100 µM L-glutamate, and after treatment with 100 µM L-glutamate in presence of 100 nM Pwx10 fraction, for 24 h. Cells were fixed and immunostained for the neuronal marker MAP-2 (green) and the glial marker GFAP (red), and counterstaining with the nuclear marker DAPI (blue). Vehicle and Pwx10 fraction treated cultures in the absence of L-glutamate do not display obvious degeneration of cell death. Cell death was evident in L-glutamate treated cultures, as assessed by the increased number of DAPI positive, MAP-2 and GFAP negative cells. Co-treatment with 100 nM Pwx10 fraction reversed a portion of the L-glutamate toxicity by increasing MAP-2 and GFAP expression and reducing the number of DAPI-only cells. All images are shown at 40x magnification. Scale bar: 100 µm. B: Quantification of neuronal survival (normalized to control, vehicle-treated cultures). L-glutamate significantly reduced neuronal survival, which was mitigated by co-treatment with Pwx10 fraction and 12 (100 nM) and the NMDA antagonist APV. Co-treatment with Pwx10 fraction (100 nM) and the L-glutamate transporter inhibitor TBOA or the selective EAAT2 inhibitor WAY 23 213613 did not rescue neuronal damage in L-glutamate exposed cultures, suggesting that 4-OH-IndAc3(Me_2)4(Me_2)3Arg^{2+}-mediated neuroprotection requires active L-glutamate transporters. 3-4 coverslips were assessed per treatment condition, and 100-150 cells were manually counted per treatment. Neuronal survival data is representative of 3 independent experiments (n=9) and control levels were not statistically different for normalization purposes. ***p <0.001, **p <0.01, *p <0.05, vs. control (no insult), ###p <0.001, vs. insult, &p <0.05 Pwx10 (100 nM) + TBOA (100 mM) vs. Pwx10 fraction (100 nM) + WAY 213613 (1 mM).

329x151mm (300 x 300 DPI)

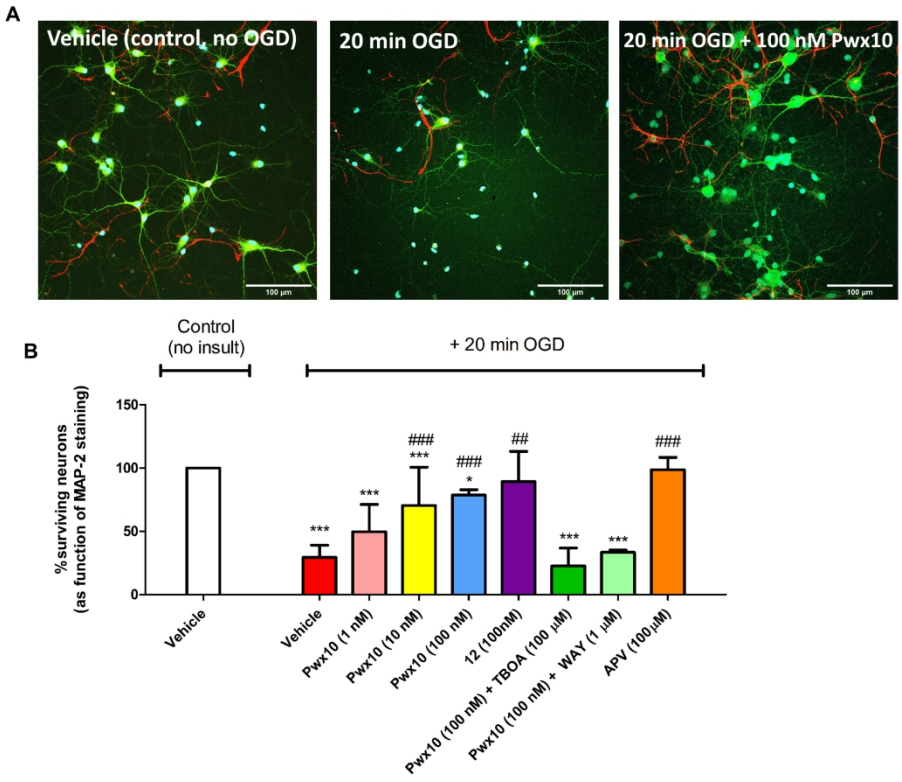

Figure 10: Neuroprotective properties of Pwx10 fraction and 4-OH-IndAc3(Me_2)4(Me_2)3Arg^{2+}; (**12**) in mixed neuron-glia cultures after transient oxygen and glucose deprivation. A. Representative Images of 14 DIV mixed neuron-glia cultures in control conditions, after 20 min OGD insult and after OGD insult followed by treatment with 100 μM Pwx10 fraction, for 24 h. Cells were fixed and immunostained for the neuronal marker MAP-2 (green) and the glial marker GFAP (red), and counterstaining with the nuclear marker DAPI (blue). Vehicle cultures in the absence of OGD insult do not display obvious degeneration of cell death. Cell death was evident after OGD insult, as assessed by the increased number of DAPI positive, MAP-2 and GFAP negative cells. Post-treatment with 100 nM Pwx10 fraction or **12** reversed a portion of the L-glutamate toxicity by increasing MAP-2 and GFAP expression and reducing the number of DAPI-only cells. All images are shown at 40x magnification. Scale bar: 100 μm. B. Quantification of neuronal survival (normalized to control, vehicle-treated cultures). OGD insult for 20 min significantly reduced neuronal survival, which was mitigated by co-treatment with 10 and 100 nM Pwx10 fraction and 100 nM **12** and the NMDA antagonist APV. The 10 and 100 nM concentration of Pwx10 fraction showed a more significant neuroprotective effect than the 1 nM concentration. Post-treatment with 100 nM Pwx10 fraction and the L-glutamate transporter inhibitor TBOA and the selective EAAT2 inhibitor WAY 23213613 did not rescue neuronal damage in L-glutamate exposed cultures, suggesting that 4-OH-IndAc3(Me_2)4(Me_2)3Arg^{2+} (**12**)-mediated neuroprotection requires active L-glutamate transporters. 3-4 coverslips were assessed per treatment condition, and 100-150 cells were manually counted per treatment. Neuronal survival data is representative of 3 independent experiments (n=9) and control levels were not statistically different for normalization purposes. ***p <0.001, *p <0.05, vs. control (no insult), ###p <0.001, vs. insult.

237x190mm (300 x 300 DPI)